Blazar Basics

Background and Time Series

Tiffany R. Lewis

NASA Postdoctoral Program Fellow

Goddard Space Flight Center, Astroparticle Physics Lab

Fermi Summer School

June 2022

tiffanylewisphd@gmail.com

Tiffany Lewis - Mini CV

Education: 2018, PhD Physics, George Mason University

Advisor: Peter Becker, GMU (with Justin Finke, NRL)

Thesis: Self-Consistent Physical Models for Blazar Jet Emission: Time Lags and Spectra for Mrk 421 & 3C 279

Employment History:

2020-present: NPP at NASA GSFC
2018-2010: Zuckerman Fellow (University of Haifa & Tel Aviv University)
2016-2018: Research Assistant GMU
2014-2016: GMU Observatory Manager

Work & Interests

- **Blazar Theory**
  - Analytic & Computational Solutions to Particle Transport Equations
  - Leptonic and Hadronic Particle Acceleration in Jets
  - Particle Energetics in the Blazar Zone
  - Connections with Data
- **AGN Theory**
  - Disk-Jet Connection
  - Line-Locking Modeling
- **Optical Observations**
  - Continuum Reverberation Mapping for AGN
  - Exoplanet Transits
  - Exoplanet Microlensing
- **Stellar Analysis**
  - Time Series Analysis of Cataclysmic Variables
- **Snowmass Community Planning**
- **Outreach & Science Communication**
- **Diversity, Equity, & Inclusion**

The Big Picture Outline

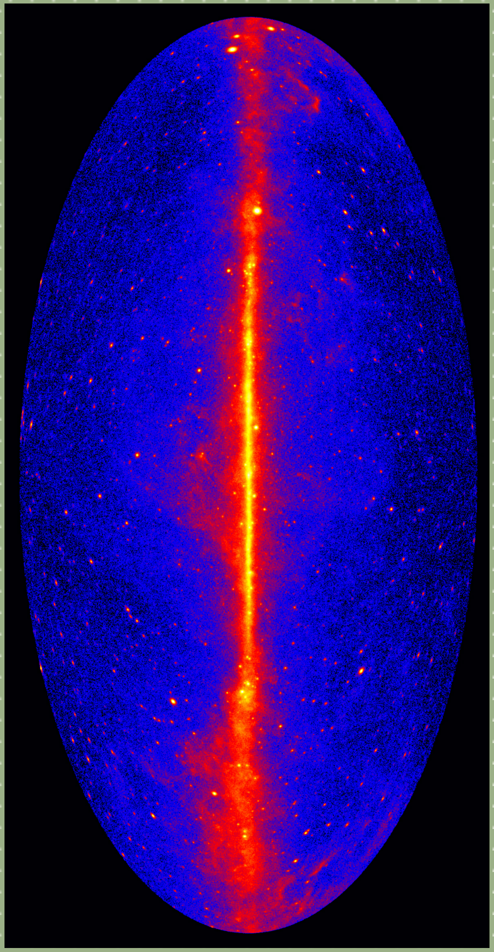

Image Credit: NASA/DOE/Fermi LAT Collaboration

- AGN & Jetted Galaxy Structures
- Discussion of the Physics of Blazar Jets
- Time Series Data
  - Light curves
  - Time Series Spectra
  - Polarization
  - Power Density Spectra
  - Time Lags (with an analytic model)
- (Thursday) Physics Review & Spectra

My First M51

Active Galaxies

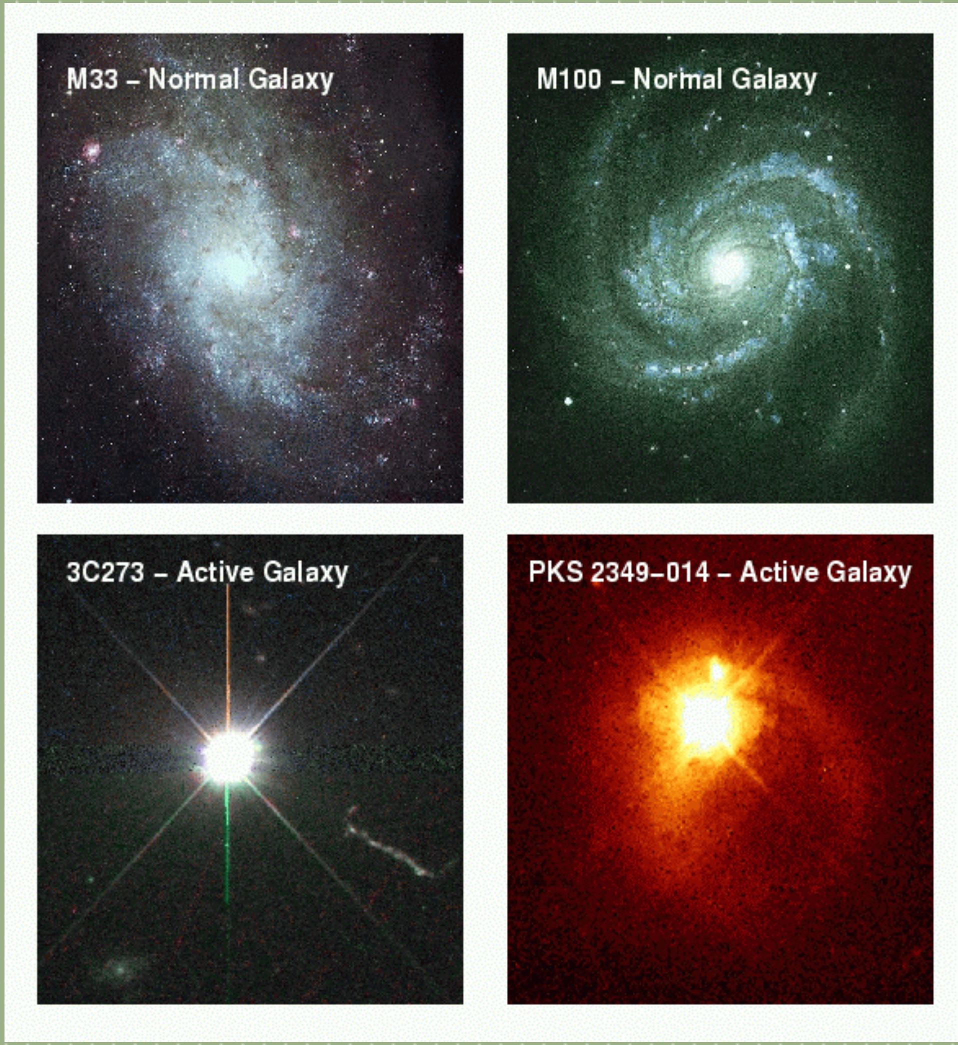

An active galaxy has a nucleus at least 100 times brighter than all the light from its stars combined.

A fraction of active galaxies have bipolar jets.

A blazar is a jetted, active galaxy, which is also pointed at Earth.

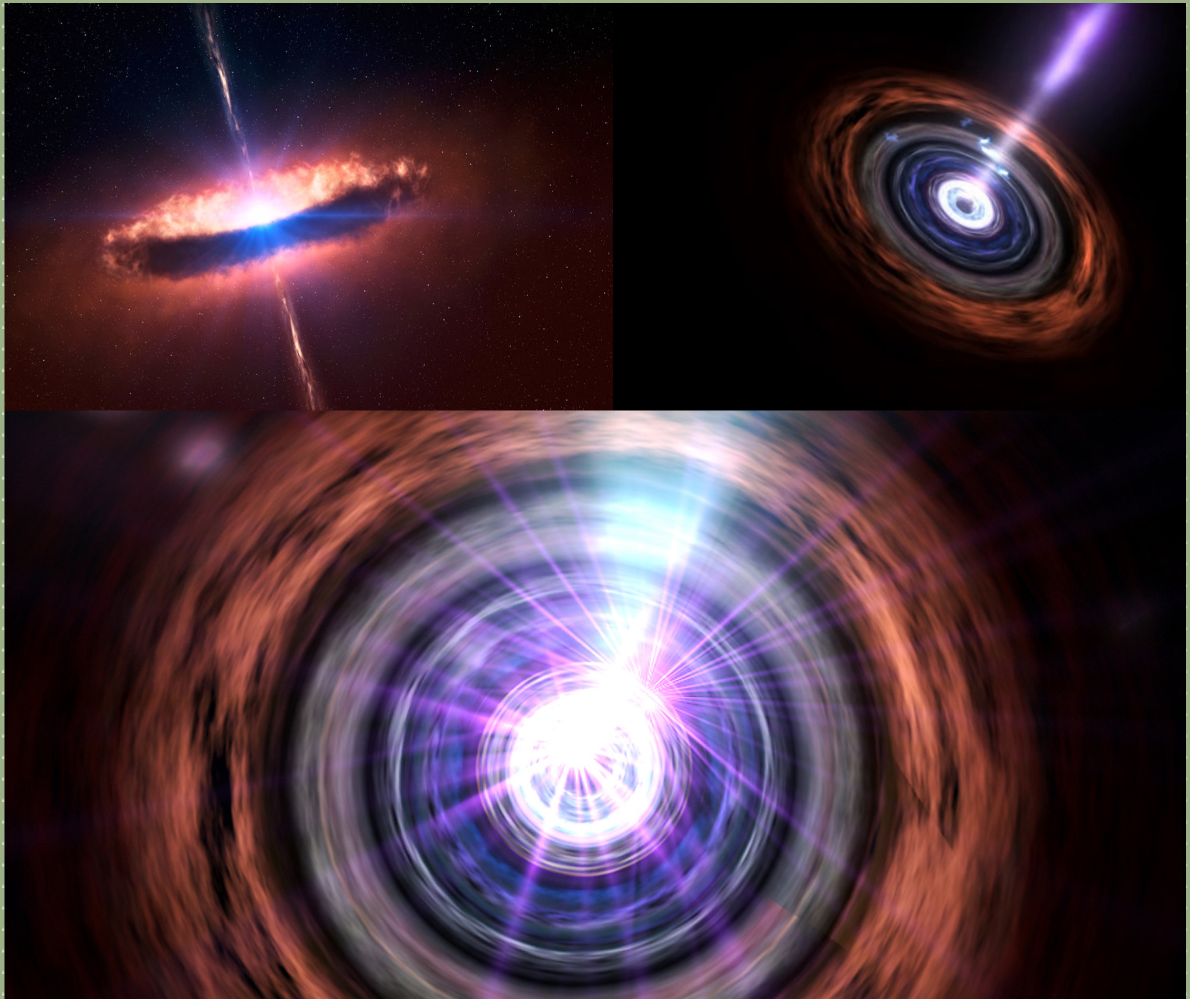

Simulation by NASA Goddard Space Flight Center Conceptual Image Lab

BL Lac's & Flat Spectrum Radio Quasars (FSRQ)

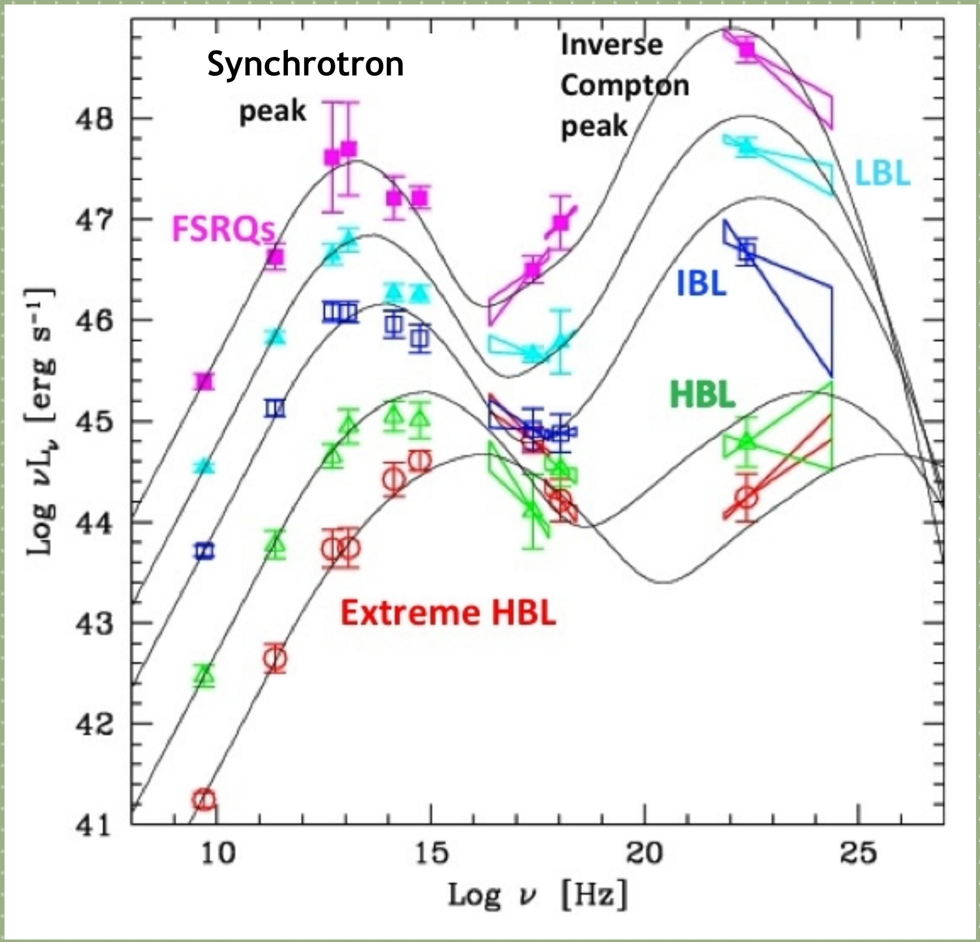

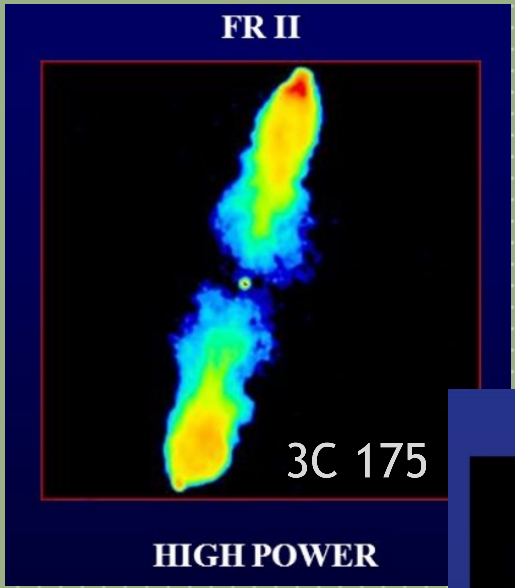

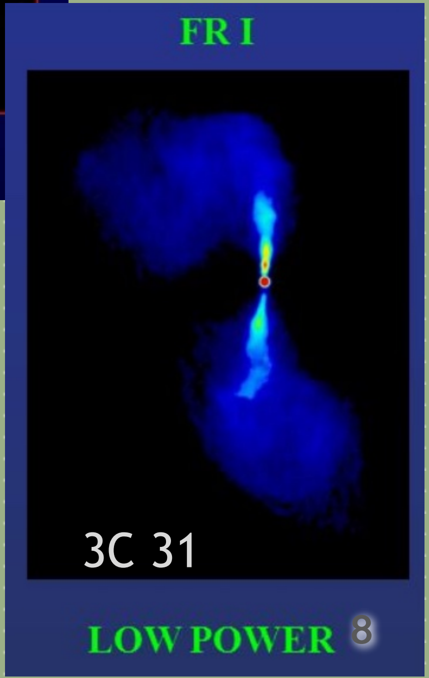

Credit:
Falomo et al.(2014) &
Fossati et al.(1998)

Blazars as an orientation of jetted AGN

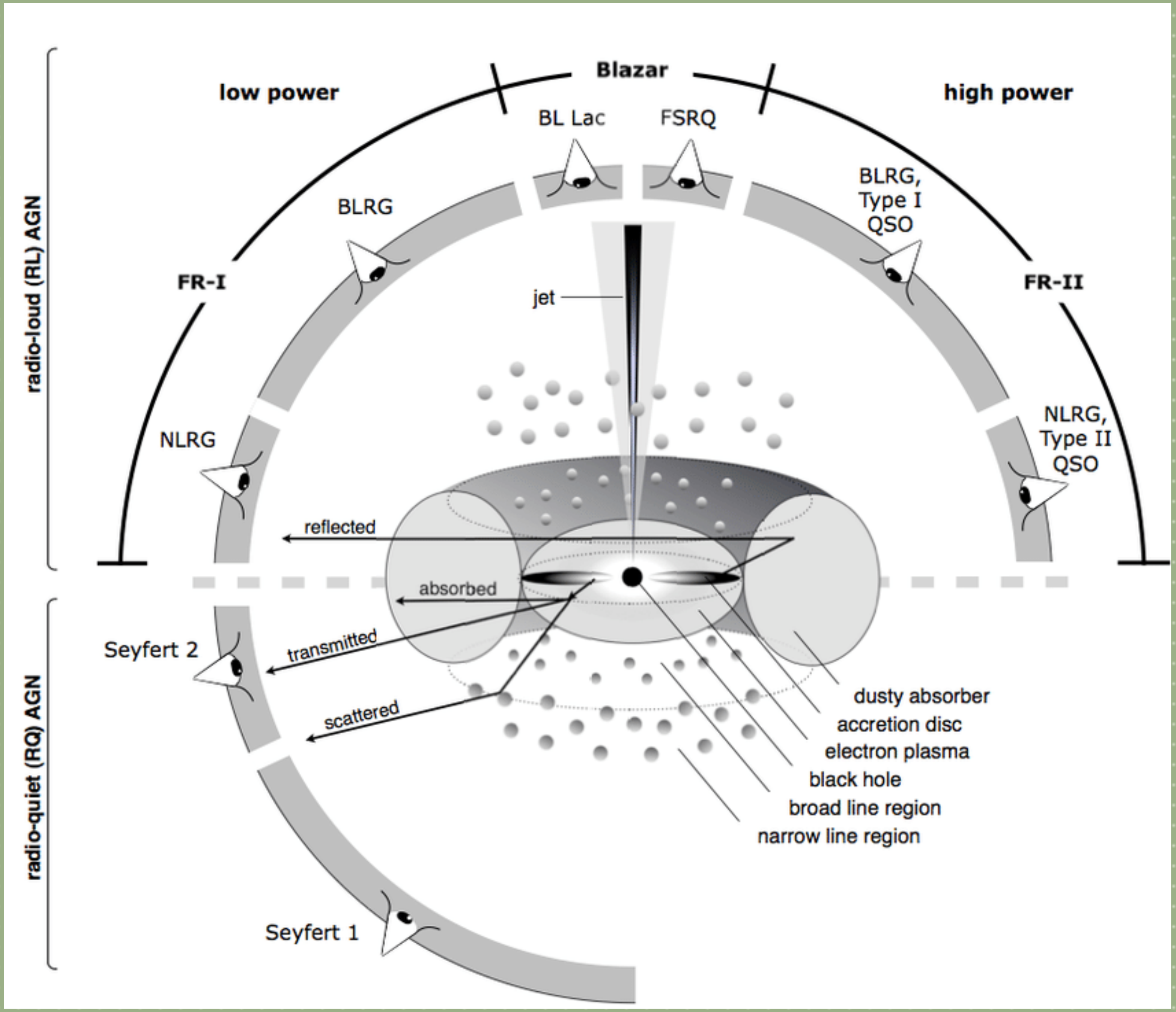

Credit: Beckmann & Schrader (2012)

Spectra & Jet Structure in Blazars

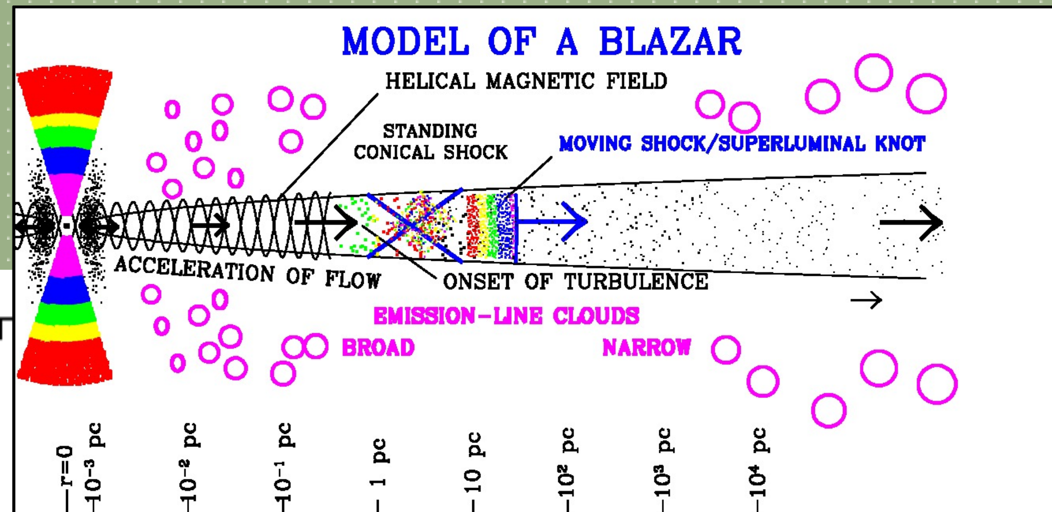

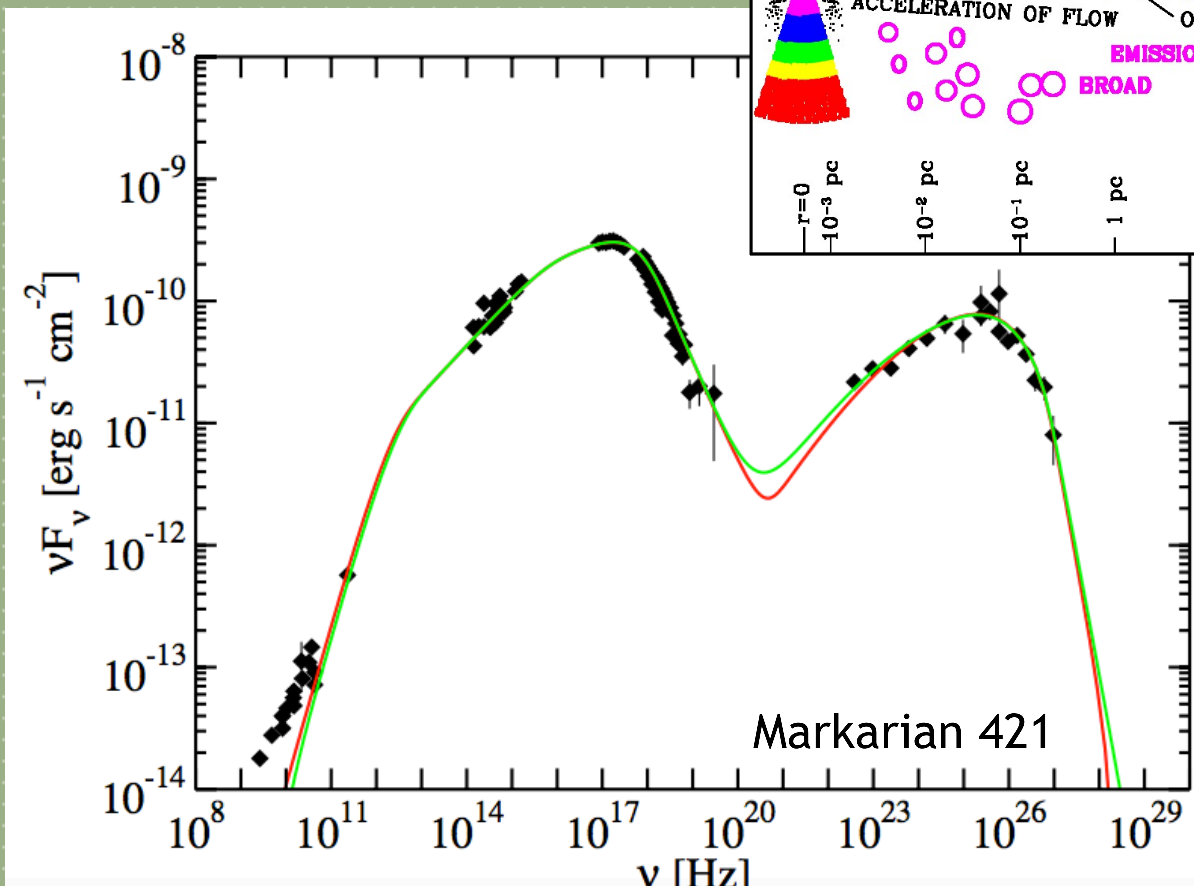

Credit: Alan Marscher, Svetlana Jorstad, et al. (top)
Abdo et al. 2011 (left)


Blazars are the most energetic sustained sources in the known Universe.
WallPaper-House (https://wallpaper-house.com/wallpaper-id-425029.php)

Background:
Physics in Blazar Jets

Particle Transport Method in Context:
every model has both strengths and limitations

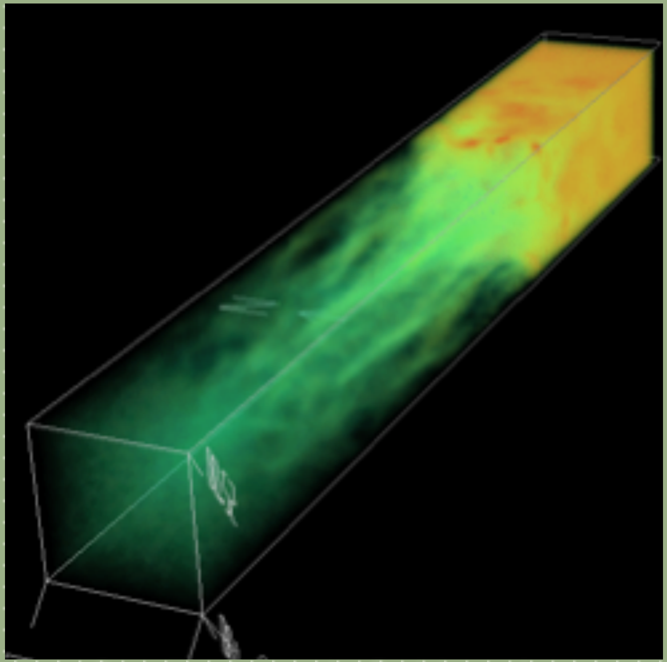

Credit: Anatoly Spitkovsky

- MHD/PIC Simulations:
  - Computationally expensive
  - Good at modeling plasma/particle microphysics
  - Difficulty producing radiation/comparing to data
- Radiative (Photon) Transport Equations:
  - Possible to compare with data
  - Cannot model acceleration
  - Not able to track particle energetics
- Particle Transport Equations:
  - Computationally efficient
  - Intuitive results
  - Historically reproduce data well

Models for Blazar Jets

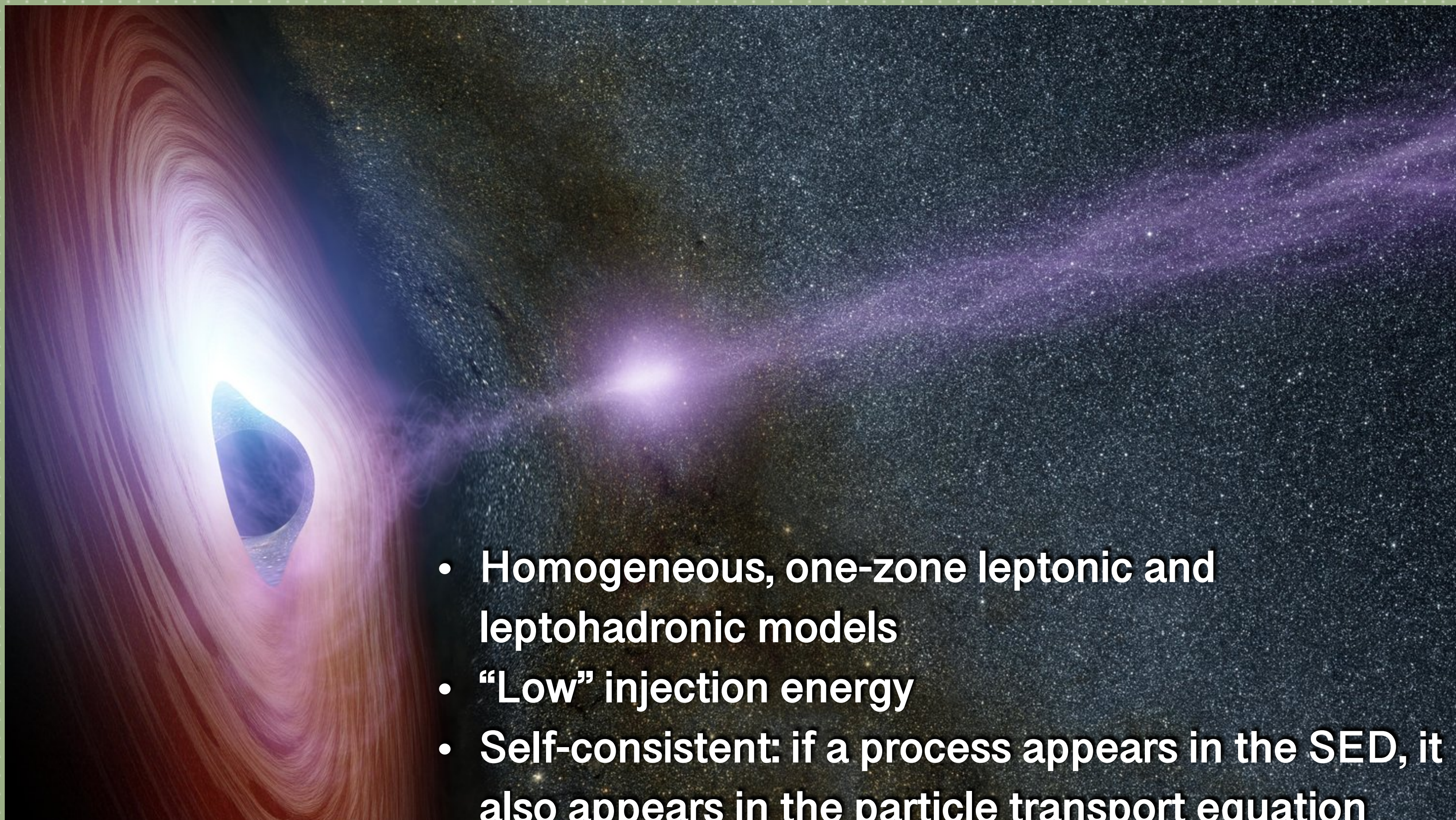

- Homogeneous, one-zone leptonic and leptohadronic models
- “Low” injection energy
- Self-consistent: if a process appears in the SED, it also appears in the particle transport equation

Image Credit: IPAC CalTech

Jet Processes

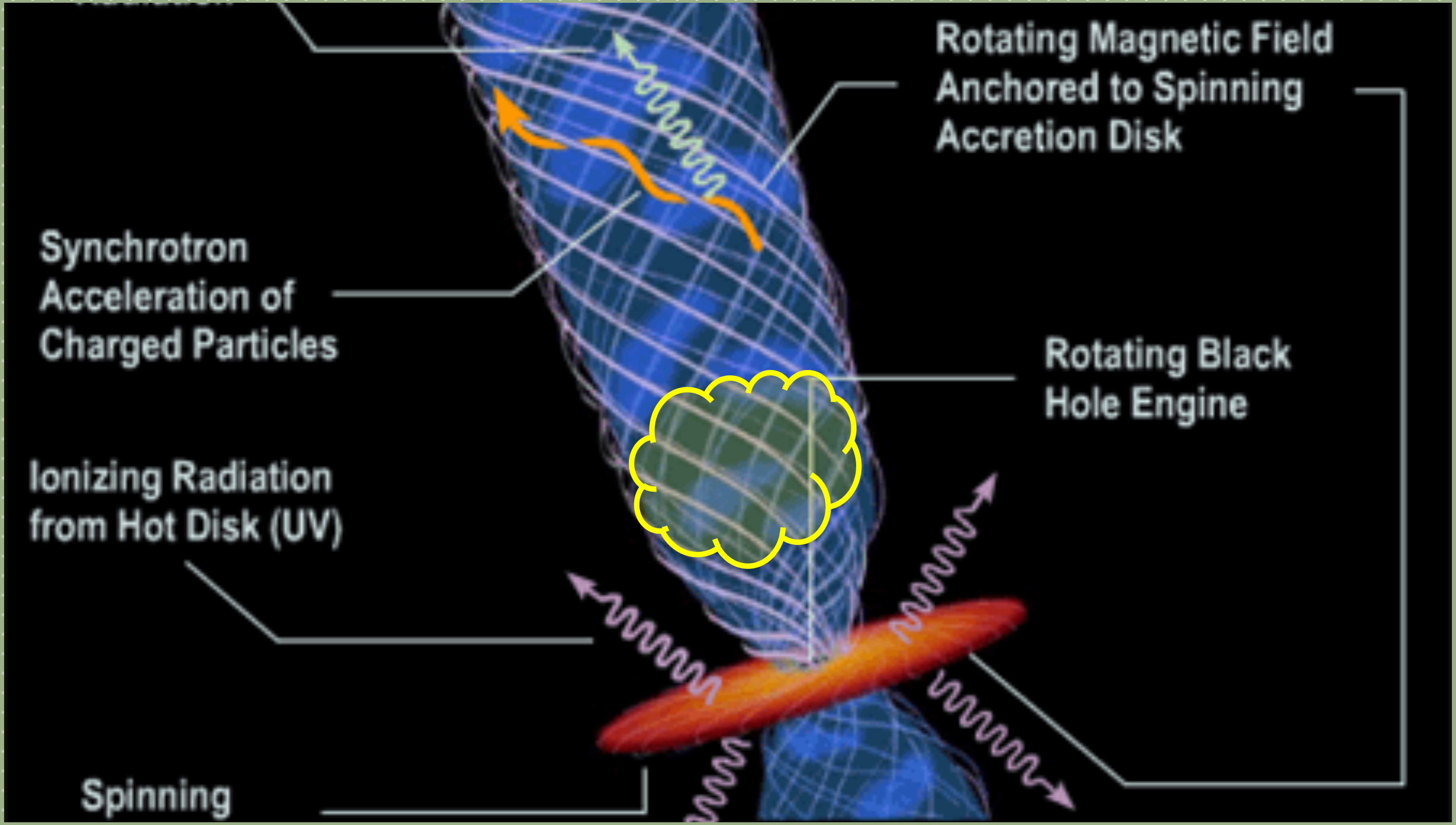

Credit: Brooks/Cole Thomson Learning

Particle Acceleration Mechanisms: 1st Order Fermi Interactions

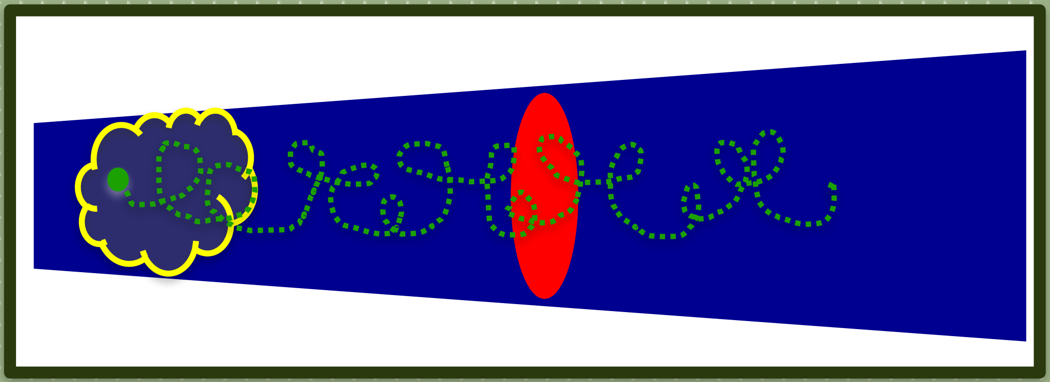

Particles gain energy from shock crossings in proportion to the energy they already have, and can pass through a shock region multiple times

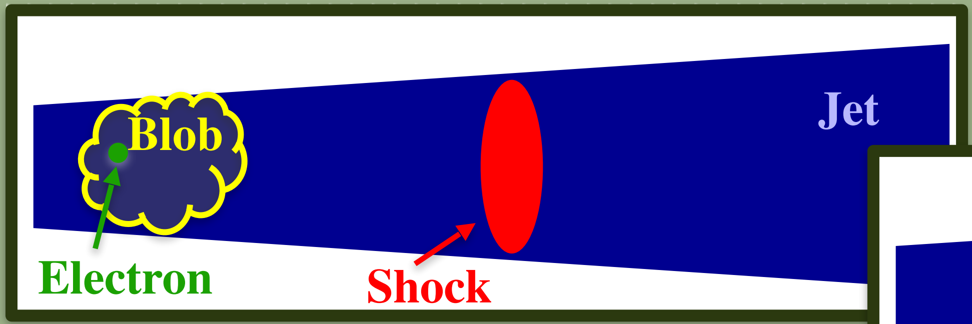

Shock Acceleration (+)
& Adiabatic Expansion (-)

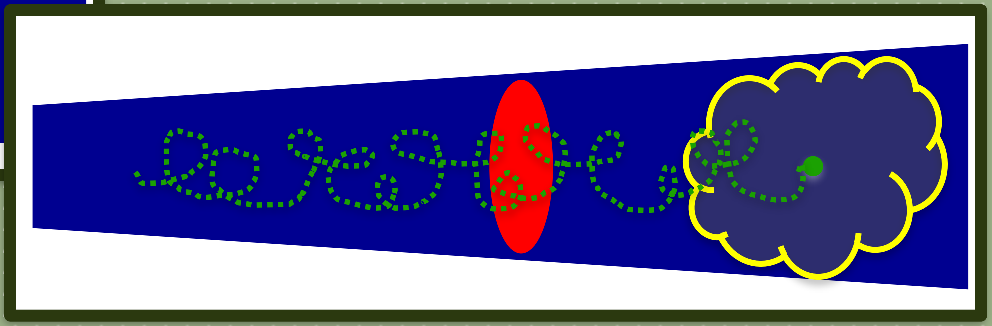

Particle Acceleration Mechanisms: 2nd Order Fermi Interactions

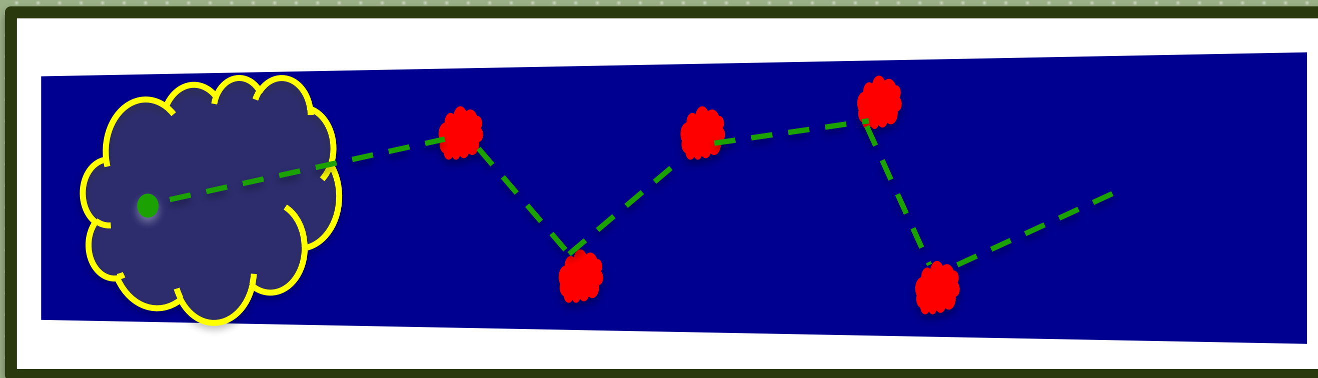

Particles always gain energy from stochastic scatterings in the head-on approximation due to the bulk motions in the jet.

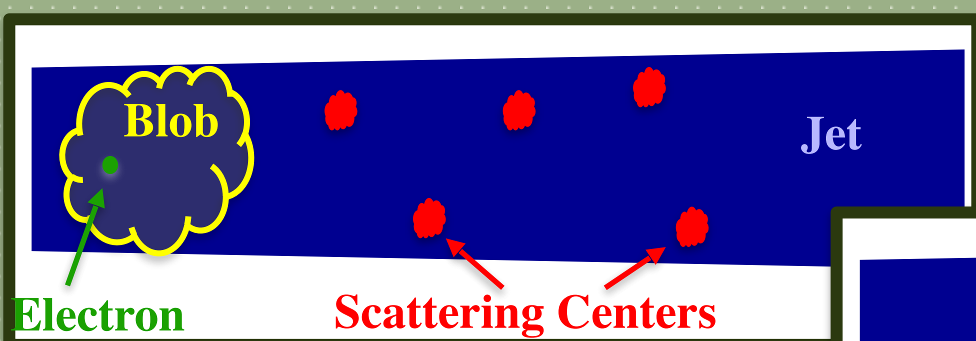

Hard-Sphere Scattering off of Stochastic MHD Waves

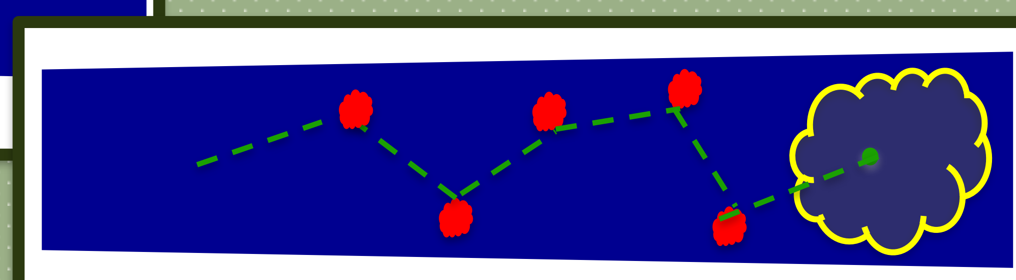

Particle Acceleration Mechanisms: Reconnection

Plasma & Field Lines flow inward

Plasma & Field Lines flow outward along the current sheet

Current Sheet

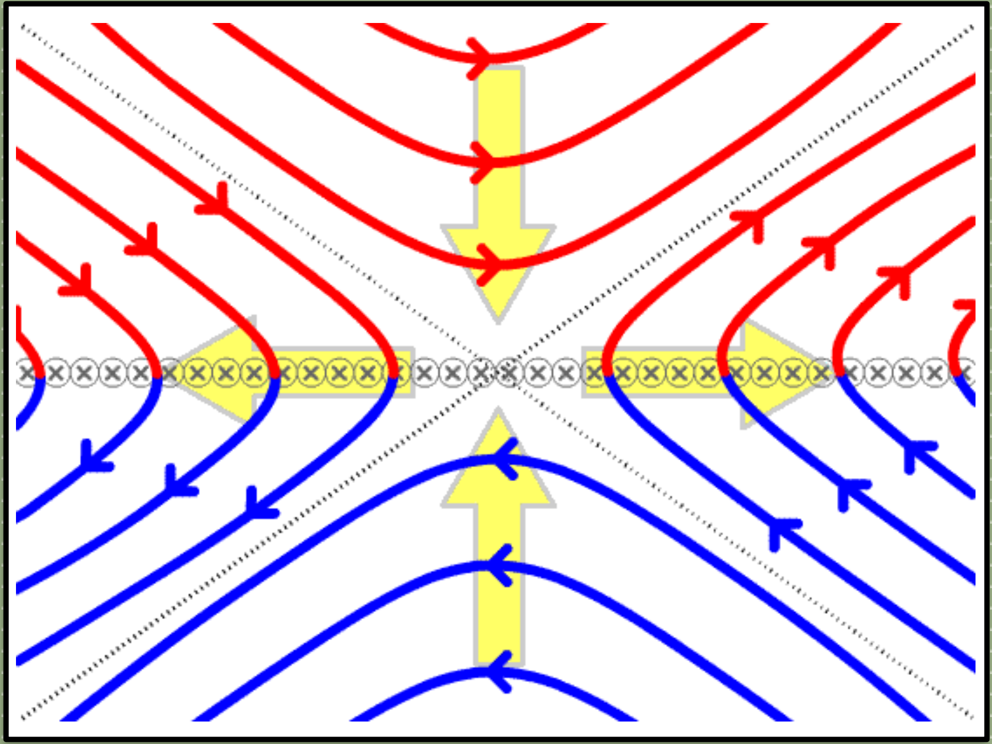

Particles gain energy from an encounter with a rapidly changing or discontinuous magnetic field that produces or strengthens an electric field.

Test Particles with Reconnection

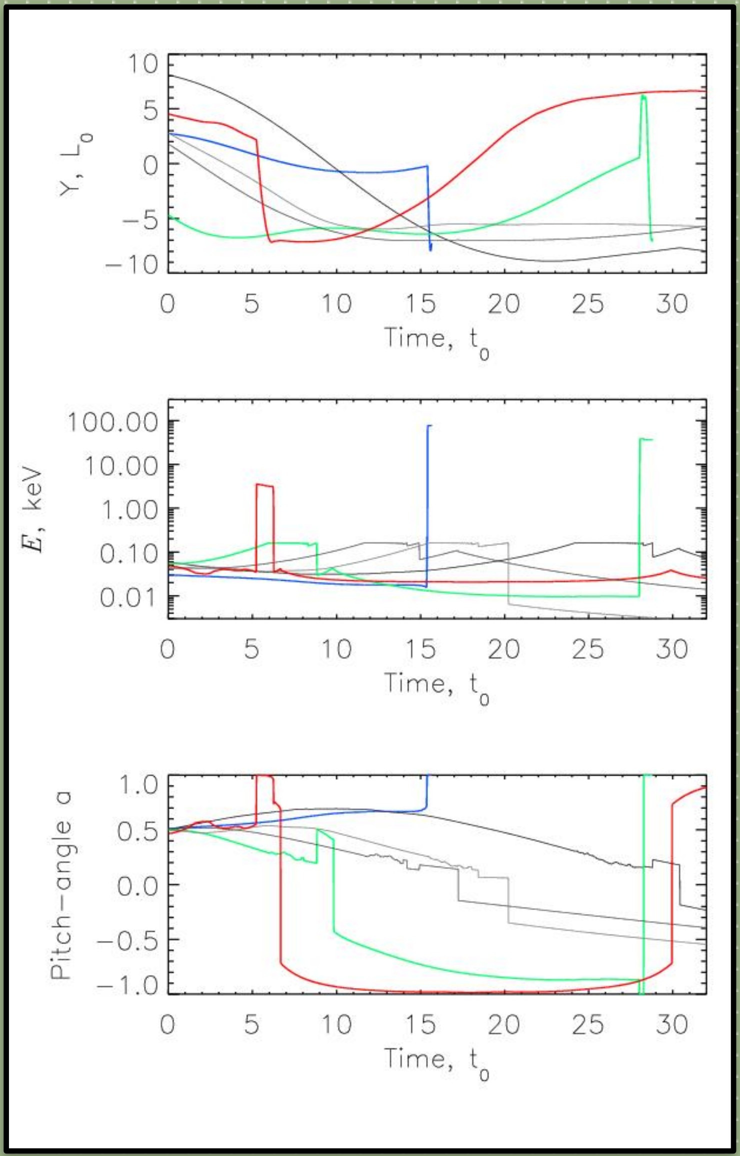

Each line represents a particle in the simulation. Three particles, denoted by red, green, and blue became nonthermal due to reconnection acceleration during the simulation.

Figure: Gordovskyy et al. (2014)

Particle Energy Loss Mechanisms: Synchrotron

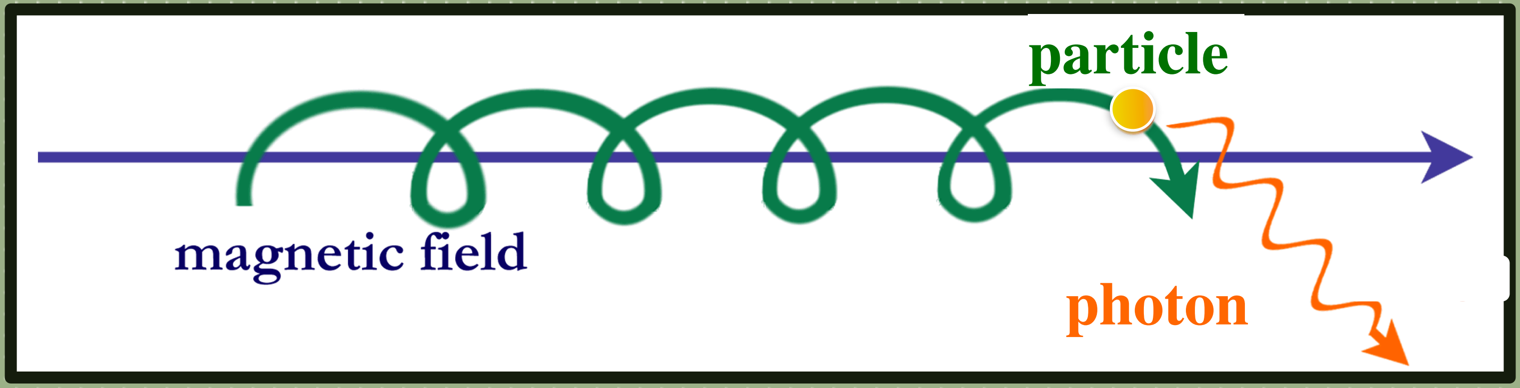

- Both electrons and protons populations can cool through synchrotron radiation.
- The rate of synchrotron cooling depends on the strength of the magnetic field.

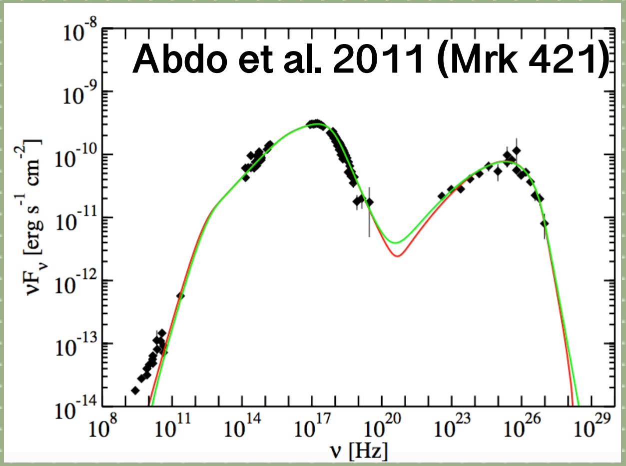

Illustration: CXC/S. Lee

Particle Energy Loss Mechanisms: Inverse-Compton

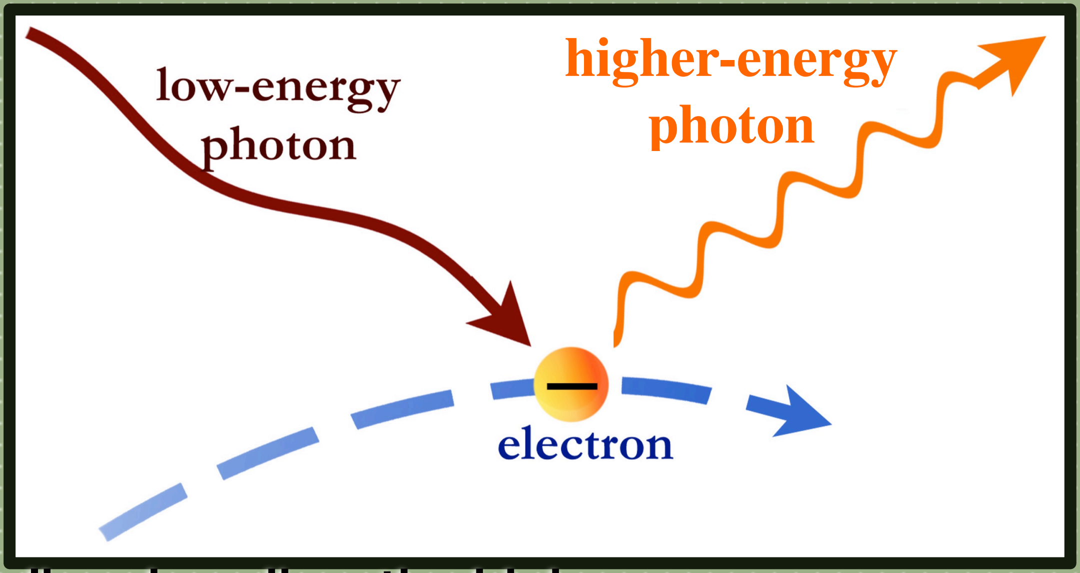

- Compton cooling describes the high-frequency SED bump in the leptonic picture.
- The Compton cooling rate depends on the energy density of the 'low-energy' photon field

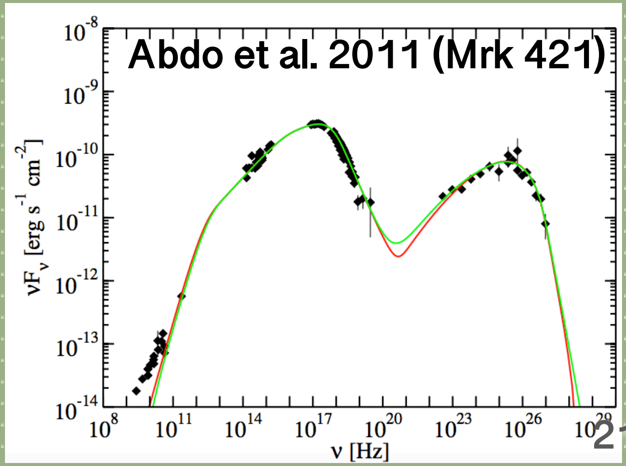

Illustrations: CXC/S. Lee

Particle Energy Loss Mechanisms: Photo-pion Production - Delta Resonance

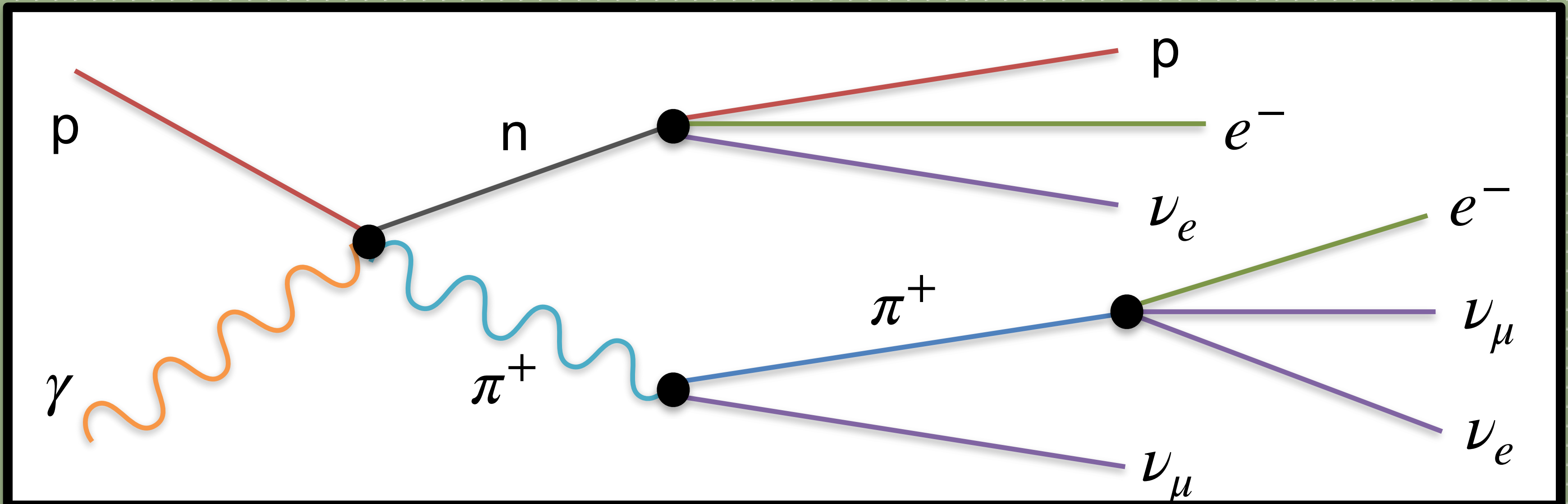

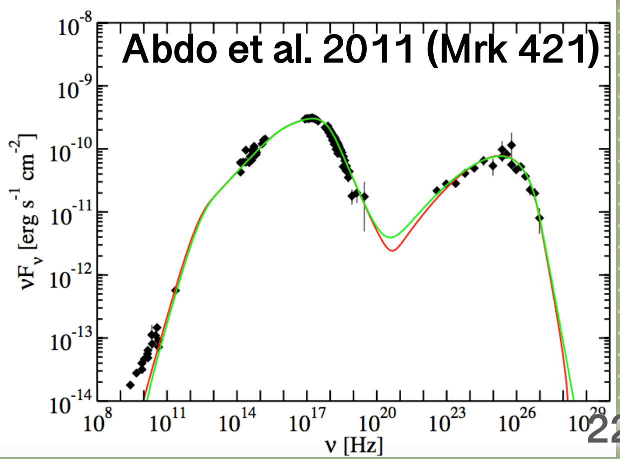

- Photo-pion production contributes to cooling for the proton population
- It also has the potential to produce observable neutrinos.

Illustration adapted from: Jonas Heinze

Time Series Data

Simultaneous Light Curves

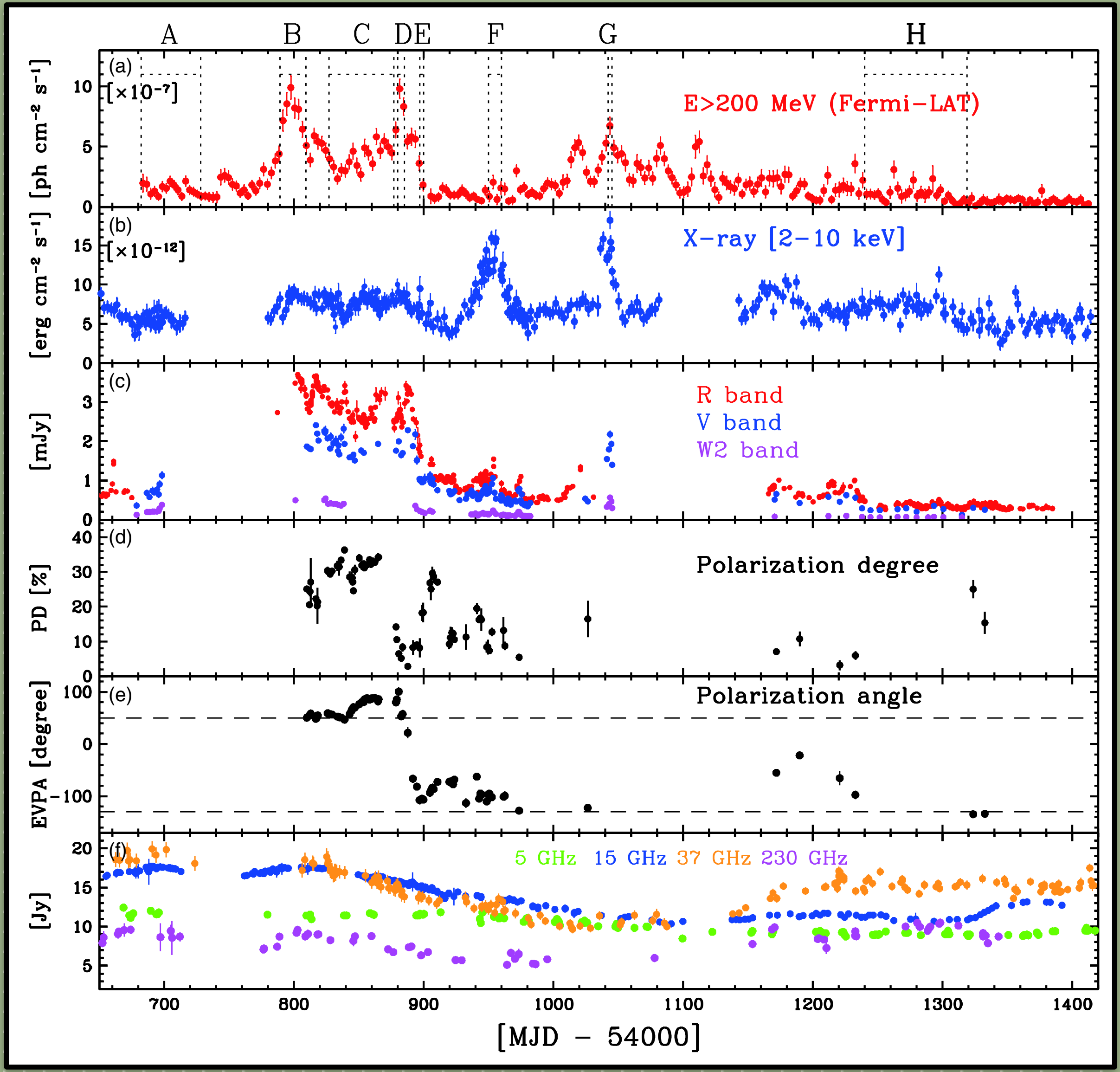

Credit: Hayashida et al. (2012)

Multi-wavelength Spectra

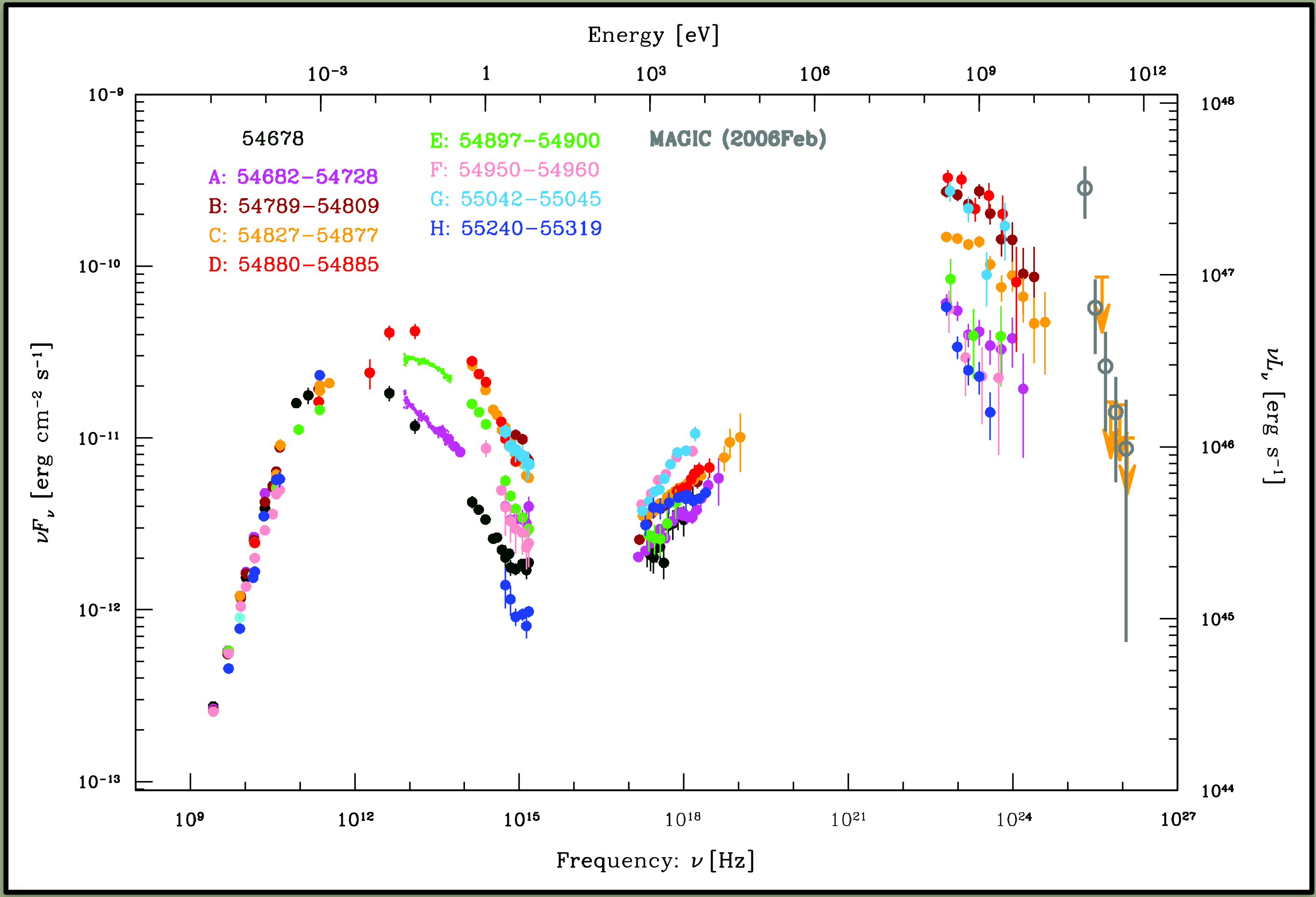

Credit: Hayashida et al. (2012)

Time Series Spectra

- 3C 279 is a bright FSRQ
- Both sides of the electron synchrotron component have limits and at times strong indications of the full shape.
- The high energy bump(s) are not as well defined due to the instrument gap in the MeV.
- The X-rays tend to indicate a slope incompatible with the GeV flux if only one log-parabola (or similar) is used. This is common for FSRQ, but there are no data to show the low-energy side of the high-energy curve or vice versa - a considerable lack of constraint for spectral models.

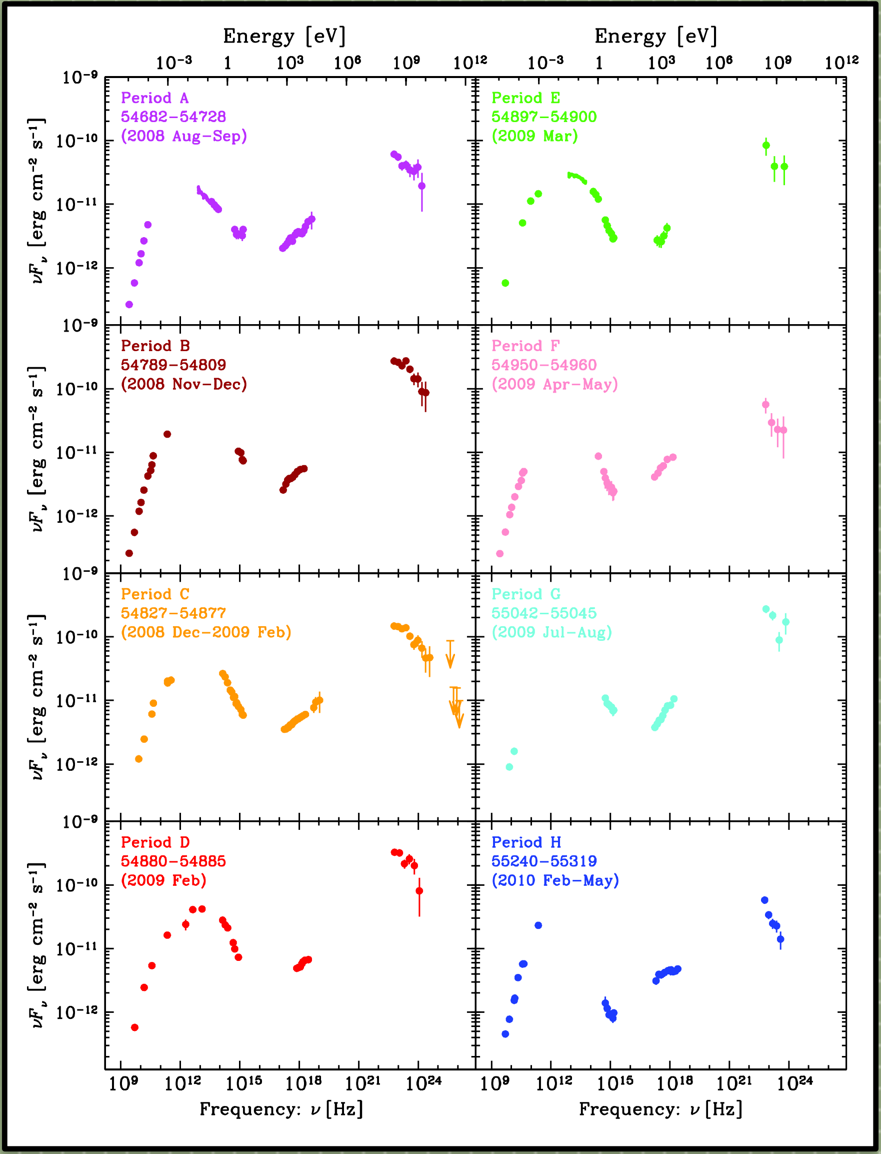

Credit: Hayashida et al. (2012)

High-Energy Polarization

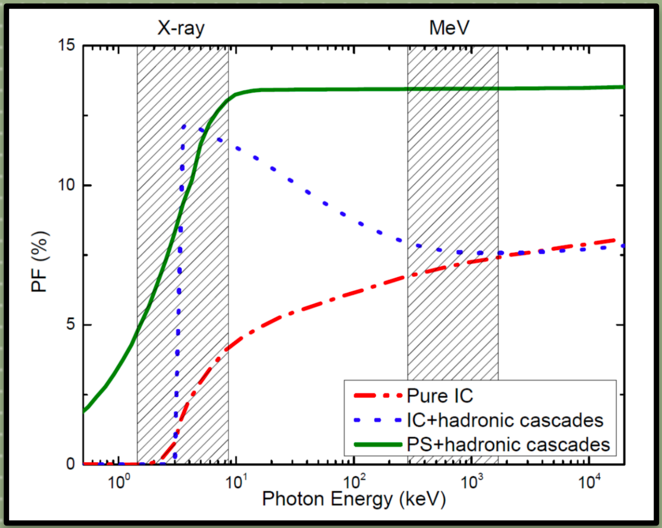

Zhang et al. (2019) polarization fraction spectrum for blazar emission mechanisms

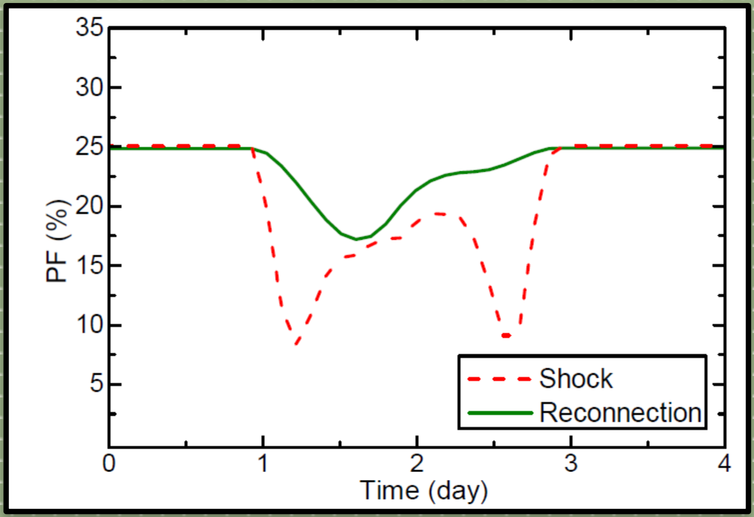

Zhang et al. (2016) polarization fraction spectrum for blazar emission mechanisms

- Optical polarization helped to confirm electron synchrotron as the source of optical emission in blazars.
- X-ray and MeV polarization measurements will similarly provide a more definitive identification for the source of blazar emission for their respective energies.

Power Spectral Density

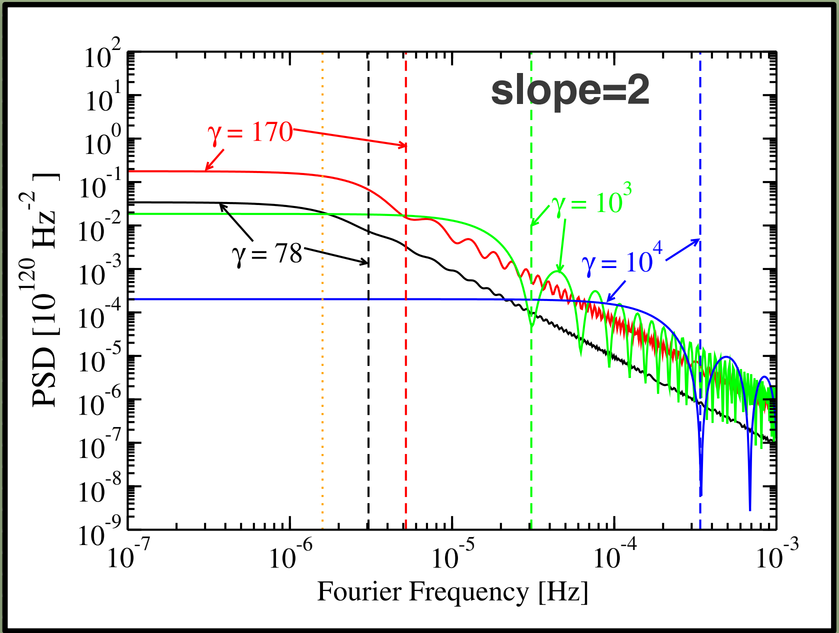

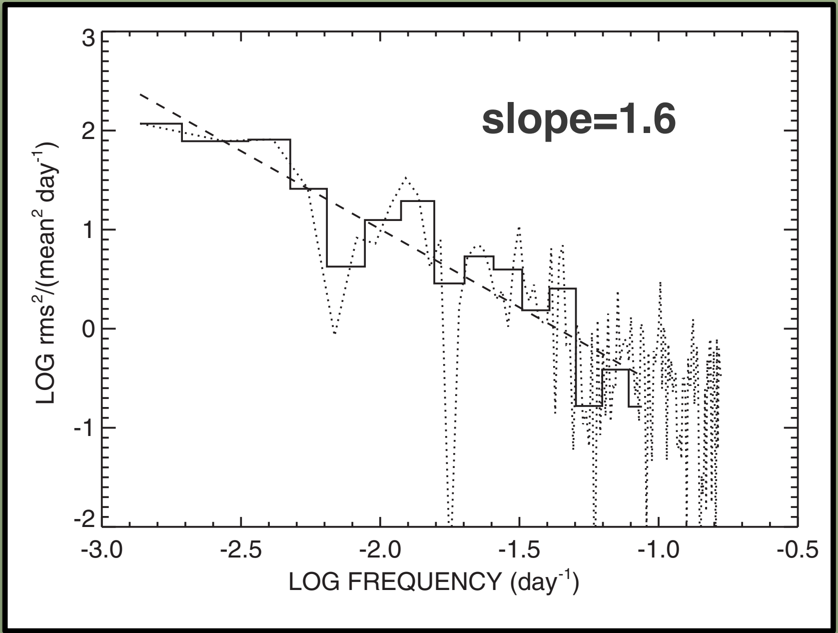

PSD simulated from an analytic model of electrons injected a power-law (shock acceleration) with an index of 2. The break frequency is related to the inverse of the particle escape timescale. For lower energies, periodic variability on timescales below the escape timescale are preferred.

Power density spectrum of the 3C 279 gamma-ray light curve (histogram is 3 day bins; dotted line is raw PDS; dashed is a linear fit to binned). Frequency is Fourier. White noise subtracted; red noise unaccounted for.

Credit: Finke & Becker (2014)

Credit: Hayashida et al. (2012)

Quasi-periodic Analysis

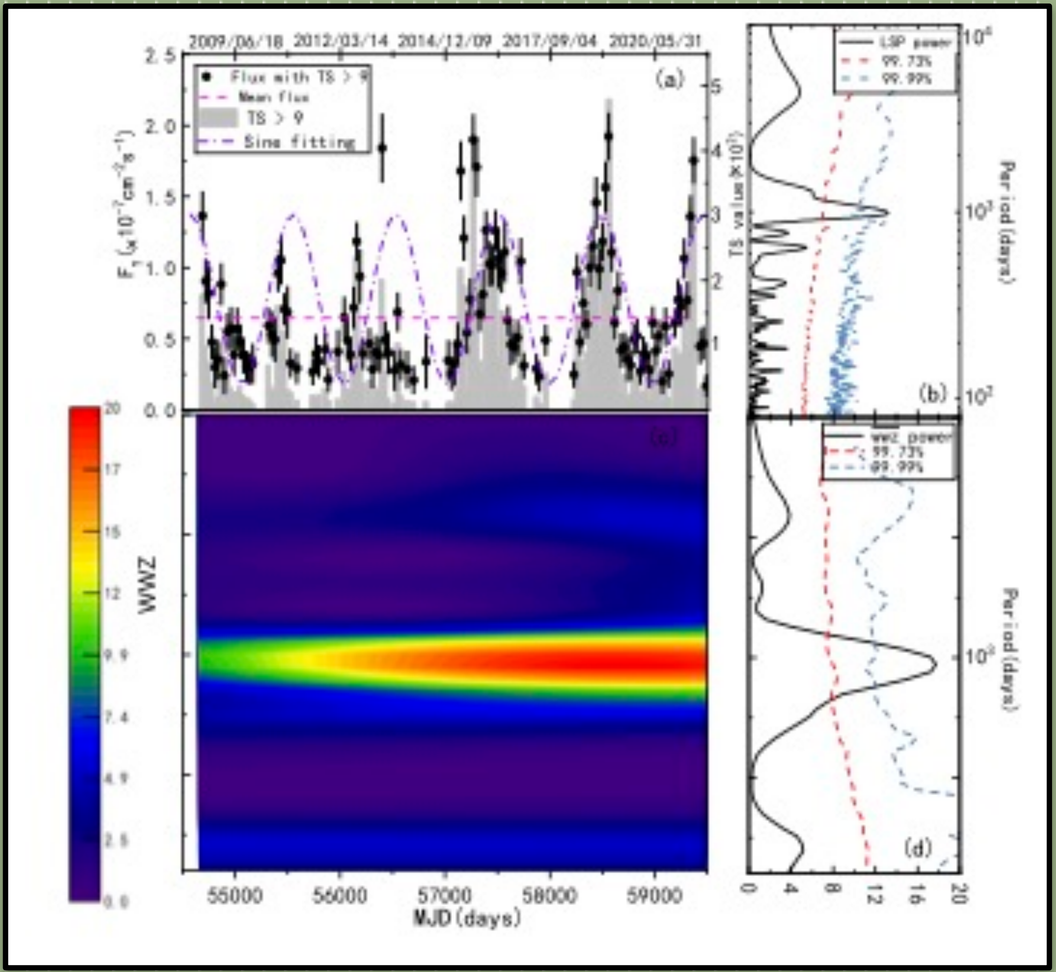

PKS 0405-385

Over 13 years of FermiLAT data, they detected a 2.8yr quasi-periodic signal with a significance of 4.3sigma.

- (a) light curve with sine fitting (controversial)
- (b) power spectrum for monthly binned gamma-ray light curve with 3 and 4 sigma significance
- (c) X-axis is time (same as the light curve. Y-axis is frequency (see right side of panel d). Contour is power spectrum.
- The wavelet weighted z transform (WWZ) power represents the intensity and duration of quasi-periodic behavior.
- (d) X-axis is the significance from panel (c) added and divided by the time. Y-axis is the period.

Credit: Gong et al (2022)

Periodic & Quasi-periodic Blazar Light Curve Interpretations

- Supermassive black hole binaries may initiate or drive AGN.
- A hot spot on the accretion disk may create a periodic input to the BH.
- A helical structure that propagates from the base of the jet outward can create a periodic signature and would also cause 180deg flips in the polarization angle. (This has been observed, but not periodically, e.g. Meyer et al. 2017?)
- The kink-instability model (Zhang et al.) predicts quasi-periodicity with anti-correlated polarization.

Small Scales & Fast Variability

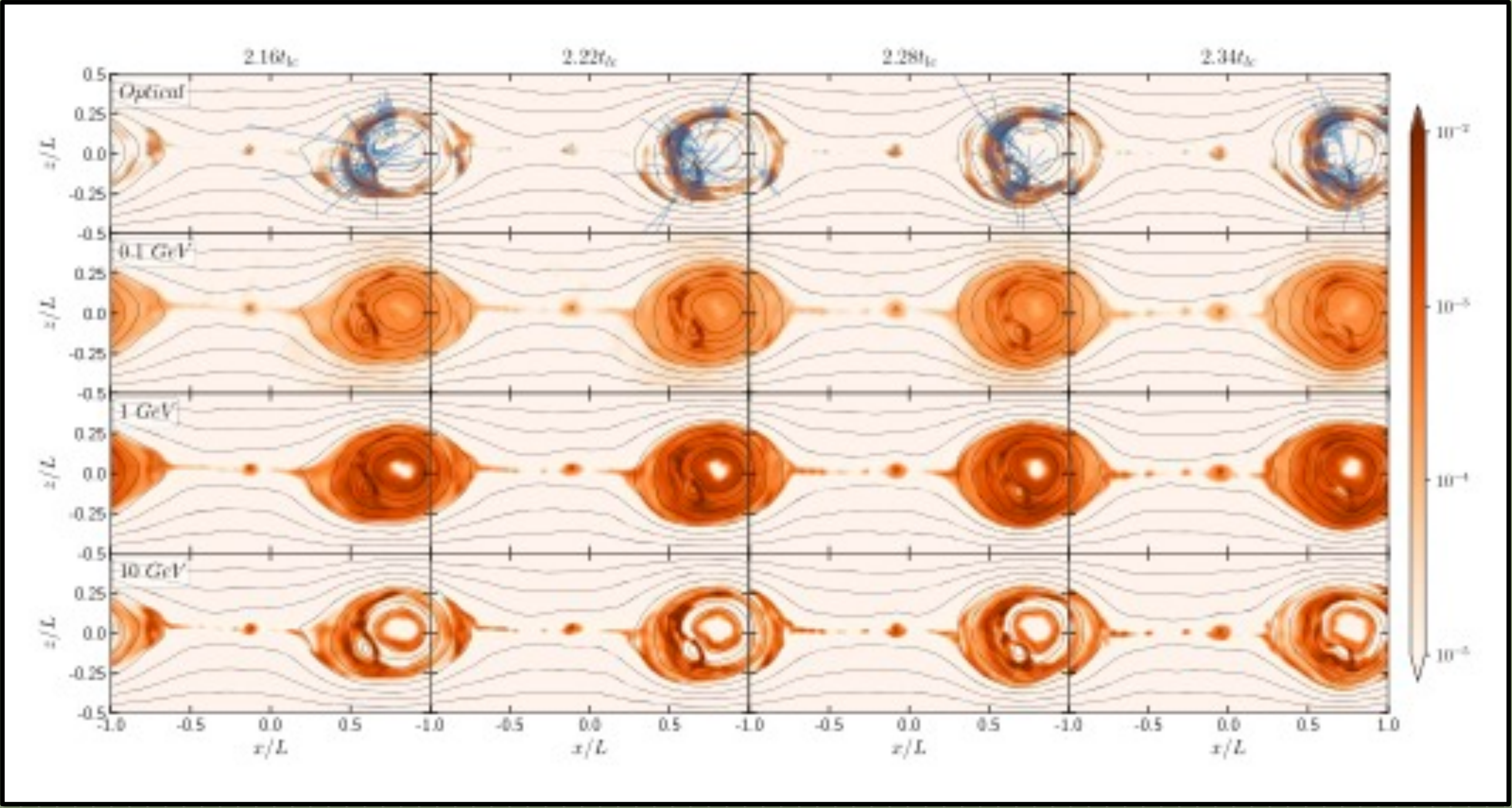

Credit: Zhang et al. (2022)

Observable Phenomena: Time Lags

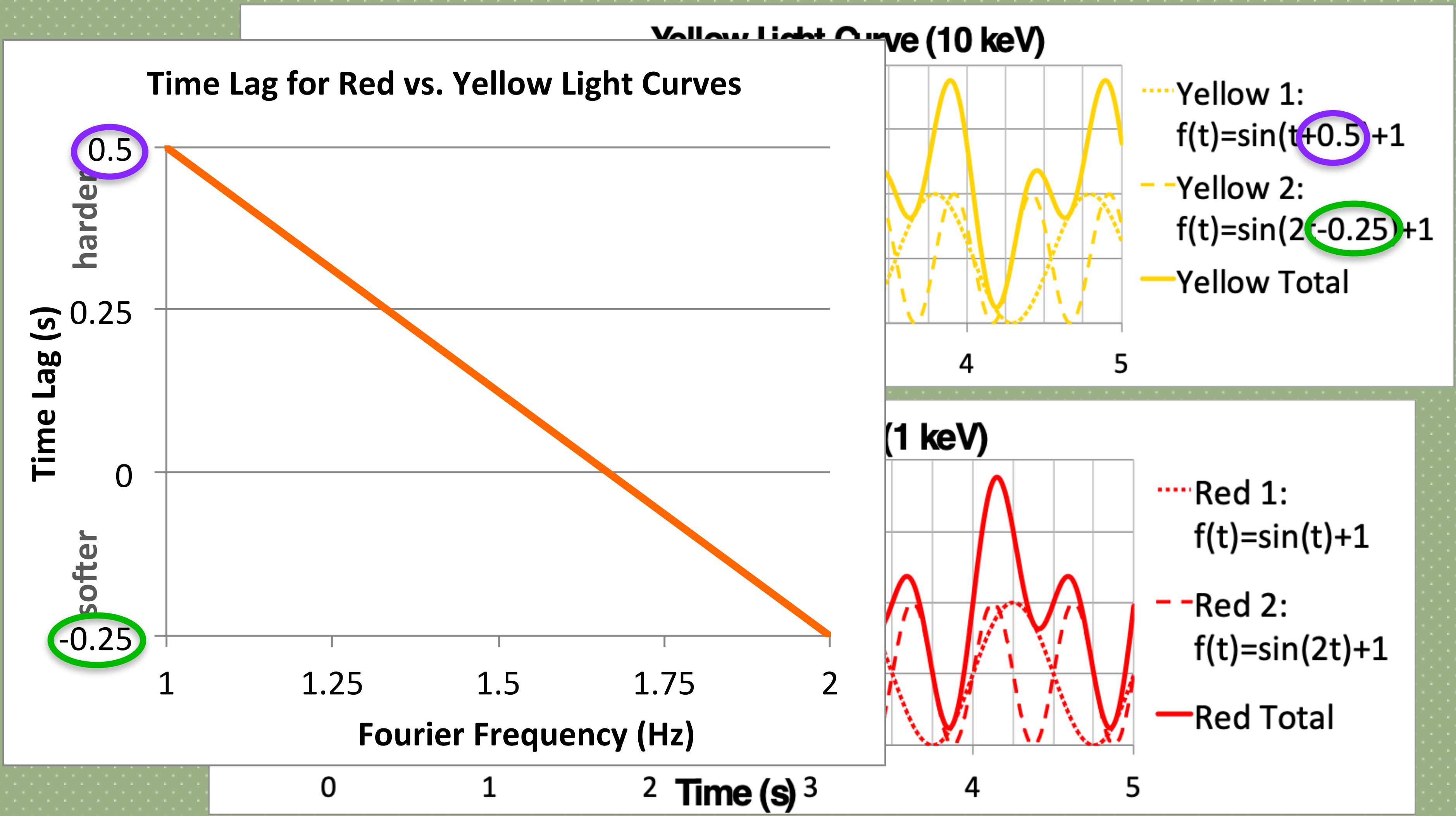

$$f(t) = A \sin(\omega t + \phi) + f_0$$

X-Ray Time Lags for Mrk 421

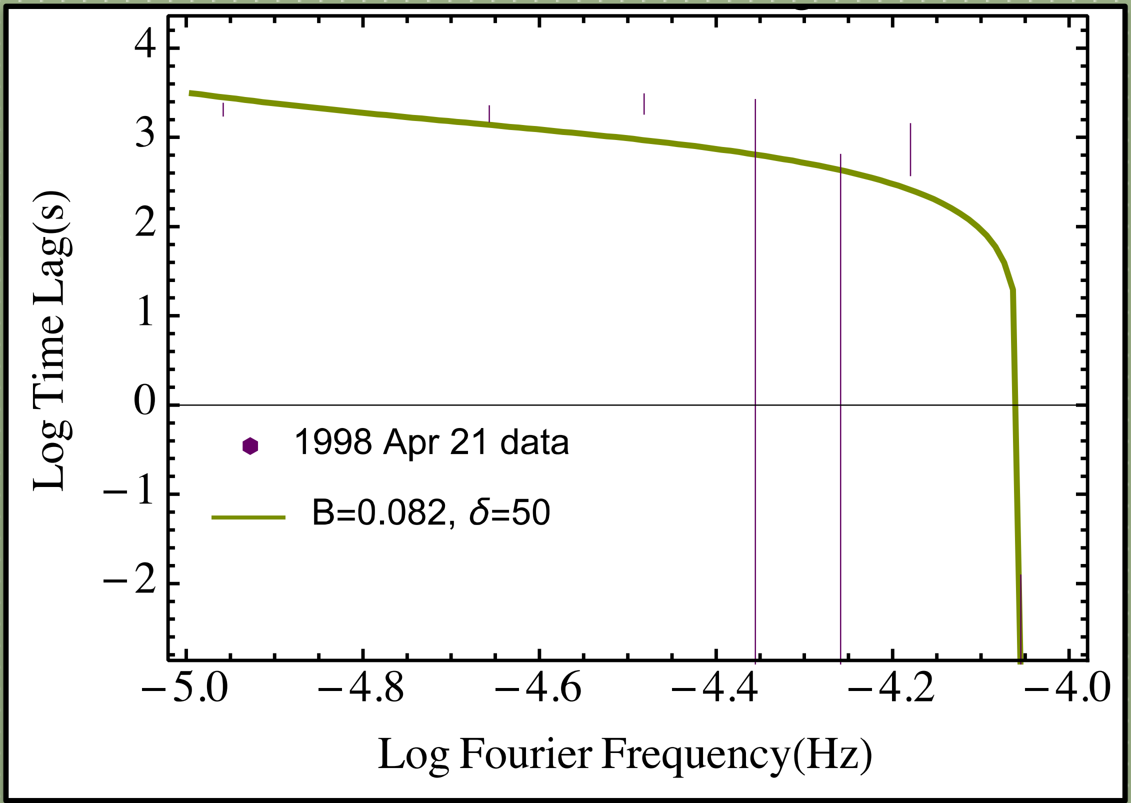

Data: BeppoSAX Zhang (2002)

Lewis, Becker, & Finke (2016)

Photon flux transform

$$G(\epsilon,\omega) = \frac{(1+z)\delta_{\rm D}^3}{6\pi d_L^2} \frac{N_{\rm inj}\, c\, \sigma_{\rm T} U_B \gamma'^3 e^{i\omega' t'_0} e^{b(\gamma'_{\rm inj}-\gamma')/2}}{b D_0 \gamma'^2_{\rm inj}} \times \frac{\Gamma(\mu-\kappa+1/2)}{\Gamma(1+2\mu)} \left(\frac{\gamma'}{\gamma'_{\rm inj}}\right)^{a/2} M_{\kappa,\mu}(b\gamma'_{\rm min})\, W_{\kappa,\mu}(b\gamma'_{\rm max})$$

Mrk 421 Modeled Light Curve to Demonstrate Time Lags

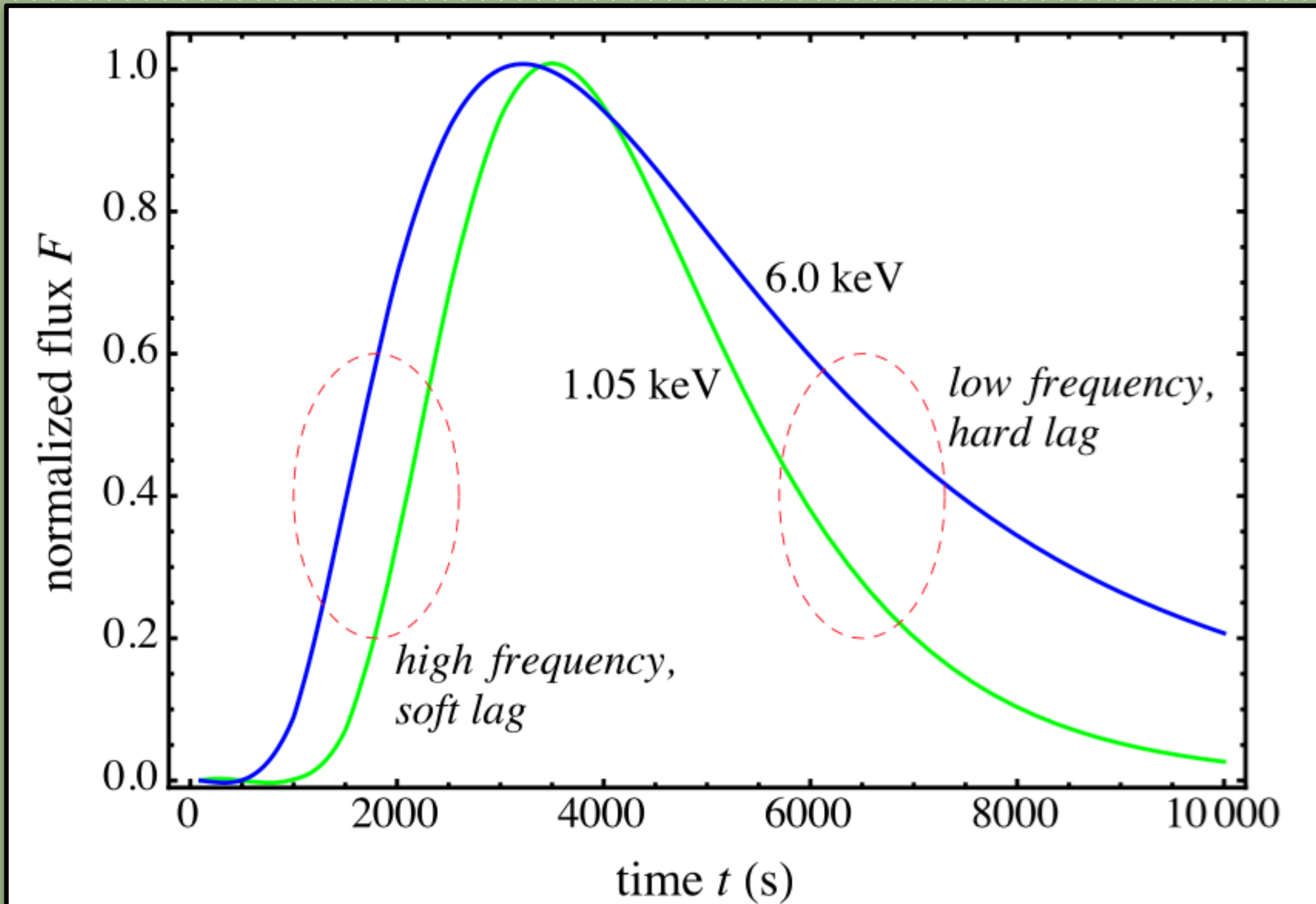

Credit: Lewis, Becker & Finke (2016)

Fokker-Planck
Electron Transport Equation

Escape Injection

$$\frac{\partial N_e}{\partial t} = \frac{\partial^2}{\partial \gamma^2}\left(D_0 \gamma^2 N_e\right) - \frac{\partial}{\partial \gamma}\left(\left\langle \frac{d\gamma}{dt} \right\rangle N_e\right) - \frac{N_e \gamma D_0}{\tau} + \left.\frac{\partial N_e}{\partial t}\right|_{\rm inj}$$

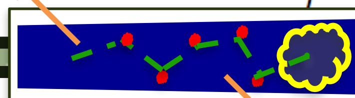

$$\left\langle \frac{d\gamma}{dt} \right\rangle = D_0\left(4\gamma + a\gamma - b_{\rm syn}\gamma^2 - b_{\rm C}\gamma^2\right)$$

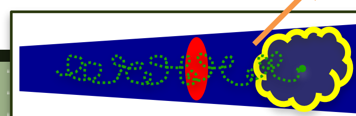

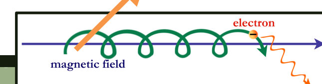

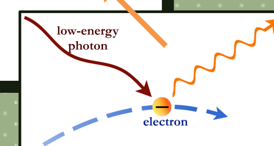

$$\left.\frac{\partial N_e}{\partial t}\right|_{\rm inj} = N_{\rm inj}\delta(\gamma - \gamma_{\rm inj})\delta(t - t_0)$$

Time-dependent

$$\left.\frac{dN_e}{dt}\right|_{\rm inj} = \dot{N}_{\rm inj}\delta(\gamma - \gamma_{\rm inj})$$

Time-independent

Injection from thermal tail

Lewis, Becker & Finke (2016)

Fourier Transform with Respect to Time

$$F(\omega) = \int_{-\infty}^{\infty} f(t)e^{i\omega t}dt$$

$$F(\omega) = \int_{0}^{\infty} f(t)e^{i\omega t}dt$$

Equivalent to Laplace Transformation if $i\omega \to s$ since there is no signal in the negative time domain

$$F_{\mathrm{G}}(\gamma,\omega) = \frac{N_{\rm inj}e^{i\omega t_0}e^{b\gamma_{\rm inj}/2}}{4\pi b D_0 (m_e c)^3 \gamma_{\rm inj}^{2+a/2}} \frac{\Gamma(\mu-\kappa+1/2)}{\Gamma(1+2\mu)} \times e^{-b\gamma/2}\gamma^{-2+a/2} M_{\kappa,\mu}(b\gamma_{\rm min})\, W_{\kappa,\mu}(b\gamma_{\rm max})$$

$$\kappa = 2 - \frac{1}{b\tau} + \frac{a}{2}$$

$$\mu = \sqrt{\frac{(a+3)^2}{4} - \frac{i\omega}{D_0}}$$

Lewis, Becker & Finke (2016)

Time-Dependent Solution & Time Lag

$$G(\epsilon, t) = \frac{2}{3}\frac{1+z}{d_L^2}\delta_{\rm D}^3 m_e^3 c^4 \sigma_{\rm T} U_B \gamma'^5 F_{\rm G}(\gamma, \omega)$$

Photon Transform

Electron Transform

G is the Fourier transform of the radiation flux produced by a particular energy of F_G

$$\delta t = \frac{\mathrm{Arg}(G_s^* G_h)}{\omega}$$

$$\mathrm{Arg}(x + iy) \equiv \tan^{-1}\left(\frac{y}{x}\right)$$

Credit: Lewis, Becker & Finke (2016)

X-Ray Time Lags for Mrk 421

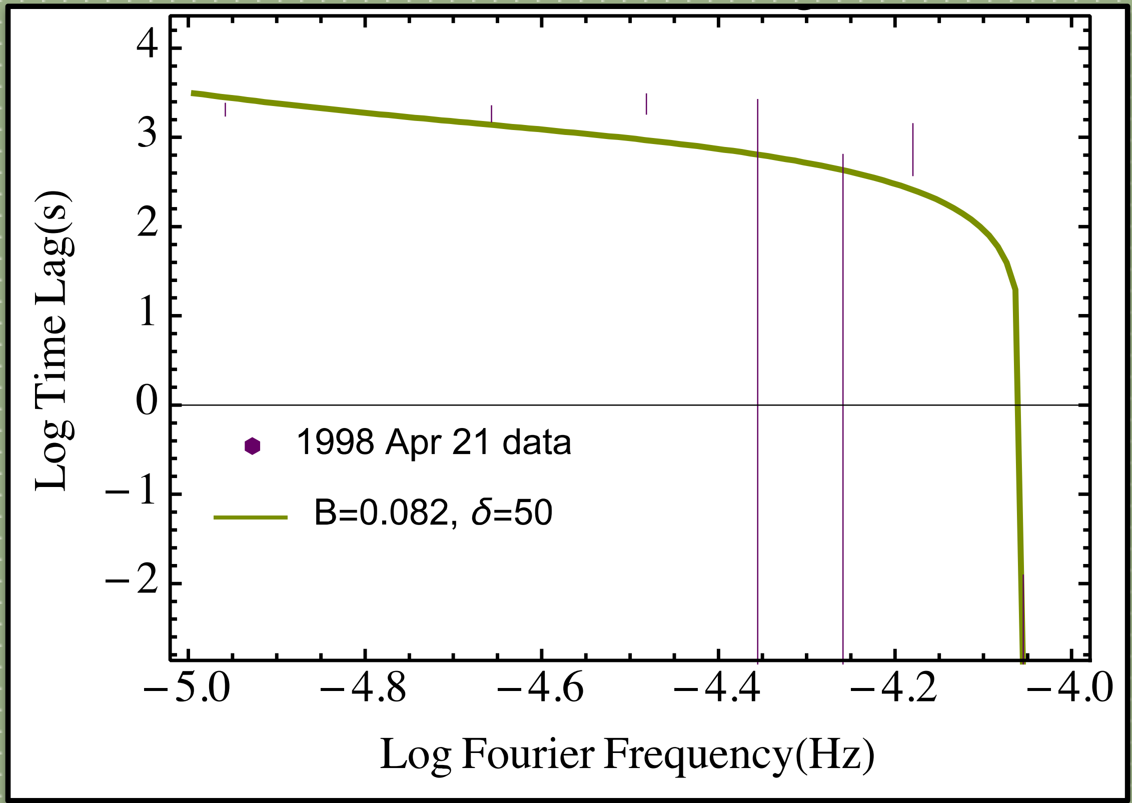

Data: BeppoSAX Zhang (2002)

Lewis, Becker, & Finke (2016)

Photon flux transform

$$G(\epsilon,\omega) = \frac{(1+z)\delta_{\mathrm{D}}^3}{6\pi d_L^2}\,\frac{N_{\mathrm{inj}}\,c\,\sigma_{\mathrm{T}}U_B\gamma'^3 e^{i\omega' t'_0}e^{b(\gamma'_{\mathrm{inj}}-\gamma')/2}}{bD_0\gamma'^2_{\mathrm{inj}}}$$
$$\times\,\frac{\Gamma(\mu-\kappa+1/2)}{\Gamma(1+2\mu)}\left(\frac{\gamma'}{\gamma'_{\mathrm{inj}}}\right)^{a/2} M_{\kappa,\mu}(b\gamma'_{\mathrm{min}})\,W_{\kappa,\mu}(b\gamma'_{\mathrm{max}})$$

Fokker-Planck
Electron Transport Equation

Escape Injection

$$\frac{\partial N_e}{\partial t} = \frac{\partial^2}{\partial \gamma^2}\left(D_0 \gamma^2 N_e\right) - \frac{\partial}{\partial \gamma}\left(\left\langle \frac{d\gamma}{dt} \right\rangle N_e\right) - \frac{N_e \gamma D_0}{\tau} + \left.\frac{\partial N_e}{\partial t}\right|_{\mathrm{inj}}$$

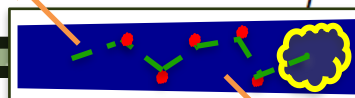

$$\left\langle \frac{d\gamma}{dt} \right\rangle = D_0(4\gamma + a\gamma - b_{\mathrm{syn}}\gamma^2 - b_{\mathrm{C}}\gamma^2)$$

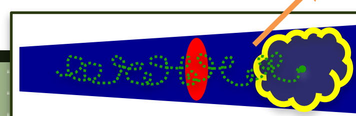

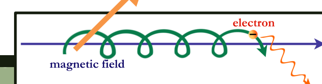

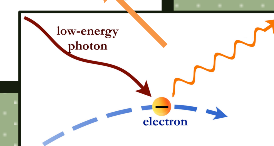

$$\left.\frac{\partial N_e}{\partial t}\right|_{\mathrm{inj}} = N_{\mathrm{inj}}\delta(\gamma - \gamma_{\mathrm{inj}})\delta(t - t_0)$$

Time-dependent

$$\left.\frac{dN_e}{dt}\right|_{\mathrm{inj}} = \dot{N}_{\mathrm{inj}}\delta(\gamma - \gamma_{\mathrm{inj}})$$

Time-independent

Injection from thermal tail

Lewis, Becker & Finke (2016)

Mrk 421 Steady-State Electron Distribution

$$N_e(\gamma) = \frac{\dot{N}_{\rm inj} e^{b\gamma_{\rm inj}/2}}{b D_0 \gamma_{\rm inj}^{2+a/2}} \frac{\Gamma(\mu - \kappa + 1/2)}{\Gamma(1+2\mu)} e^{-b\gamma/2} \times \gamma^{a/2} M_{\kappa,\mu}(b\gamma_{\rm min}) \, W_{\kappa,\mu}(b\gamma_{\rm max})$$

$$\left.\frac{dN_e}{dt}\right|_{\rm inj} = \dot{N}_{\rm inj} \delta(\gamma - \gamma_{\rm inj})$$

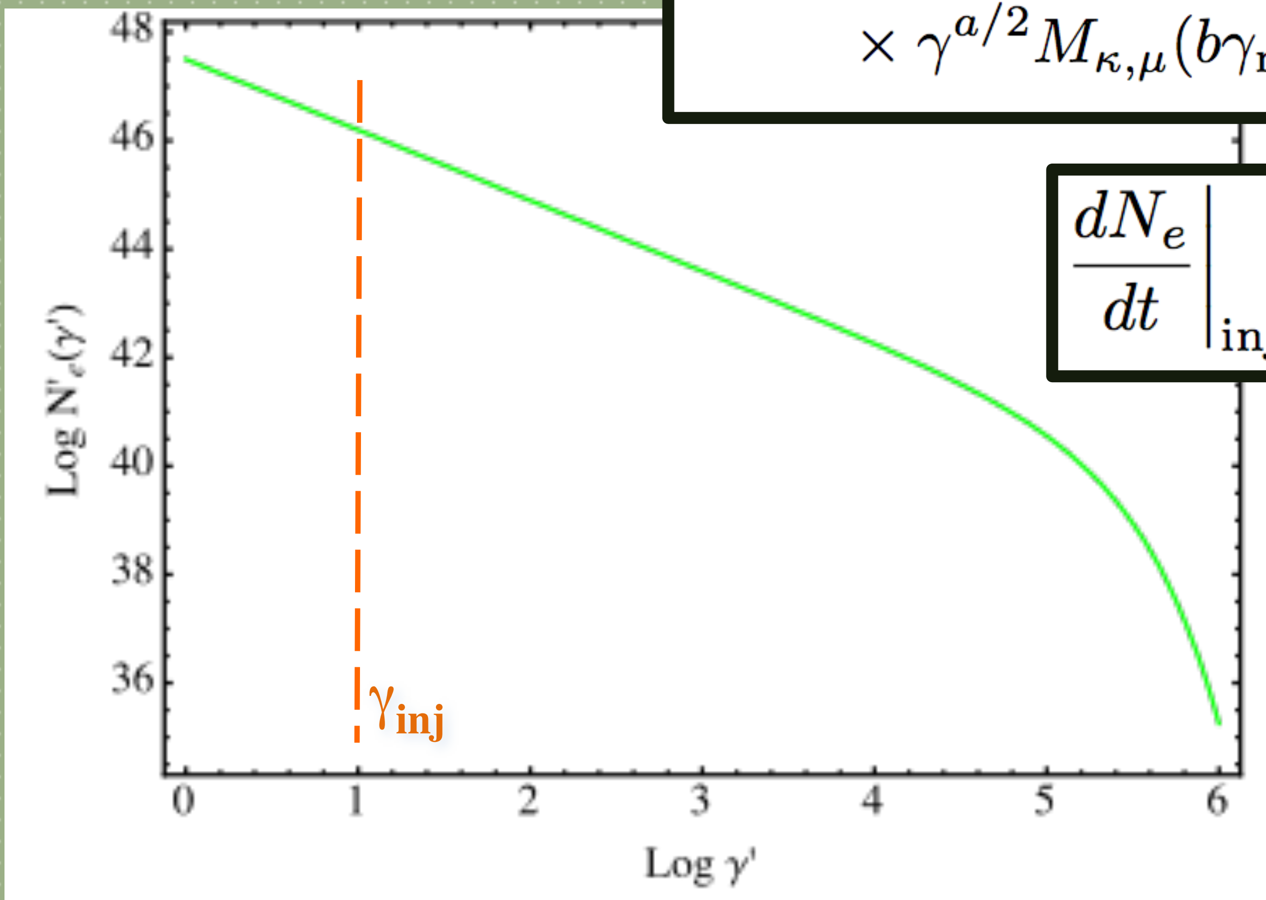

Credit: Lewis, Becker & Finke (2016)

Steady-State X-ray Spectrum for Mrk 421 (δ-approximation)

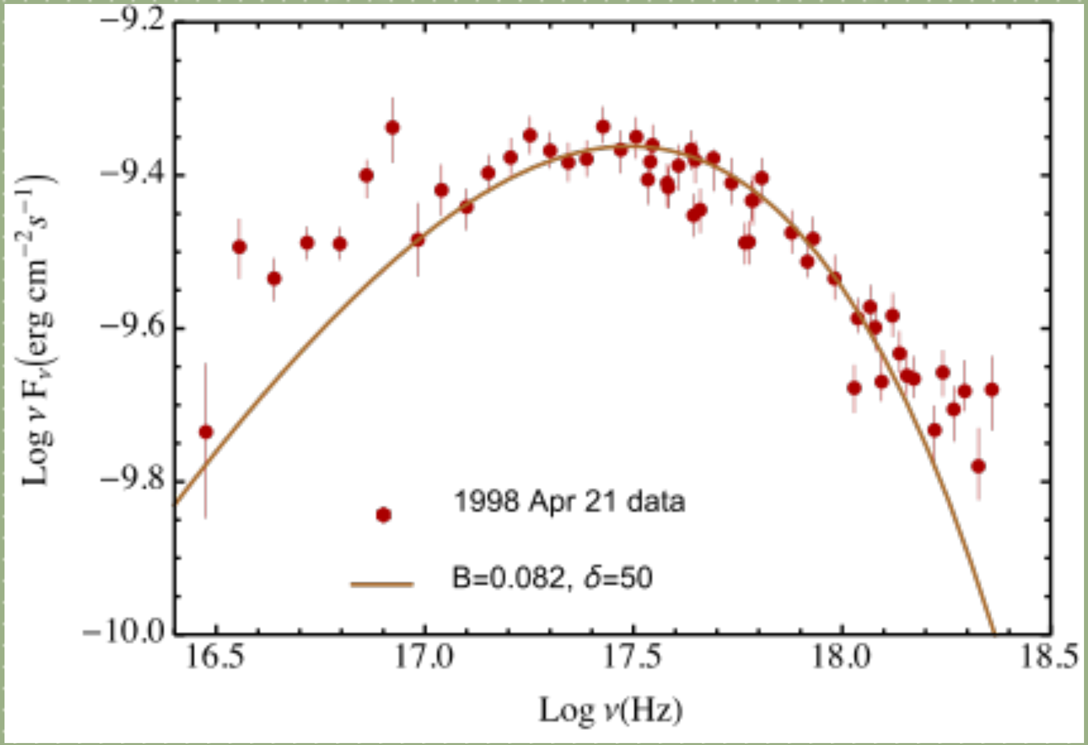

Data: BeppoSAX
Fossati et al. (2000)

Lewis, Becker, & Finke (2016)

Observed photon flux

$$\mathscr{F}(\epsilon, t) = \frac{\delta_{\mathrm{D}}^{4}}{6\pi d_L^2} c\sigma_{\mathrm{T}} U_B \gamma'^3 N_e'(\gamma', t')$$

Interpretation of Simultaneous & Self-Consistent Analysis of Mrk 421

- I analyzed each type of data product for the same flare of the same source, detected with the same instrument.
- The primary difference between the fit parameters was shock acceleration, which dominated acceleration for the time lags.
- The variable flux from Mrk 421(examining the light curve) defines the time lags, but makes up only 10% of the total flux.
- Variability in this flare was caused by the presence of a shock, where only ~10% of electrons passed through many, many times, gaining energy with each pass.
- The steady flux, produced by the other ~90% of electrons overwhelms. the smaller contribution from the shock signature in the spectrum.

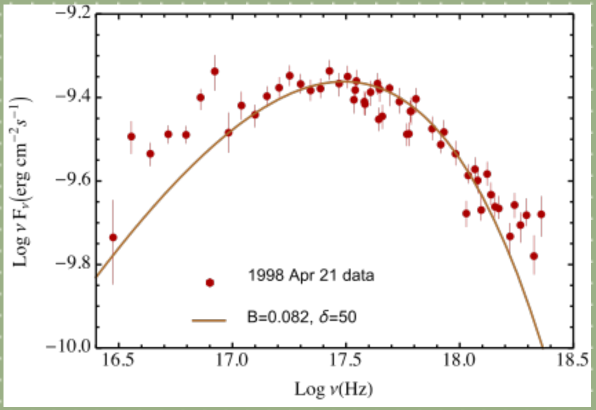

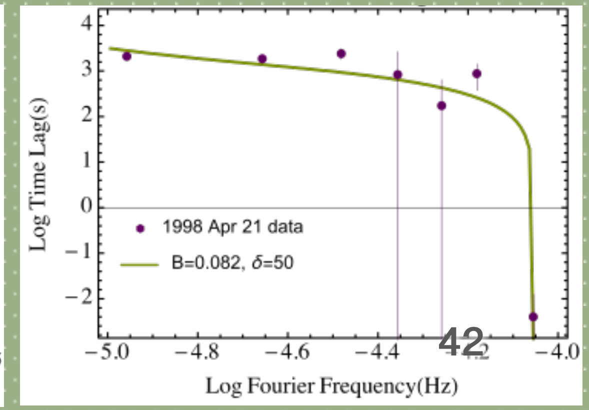

Spectral Data: Fossati et al. (2000)
Time Lag Data: Zhang (2002)
Models: Lewis et al. (2016)

Physical Picture in Markarian 421

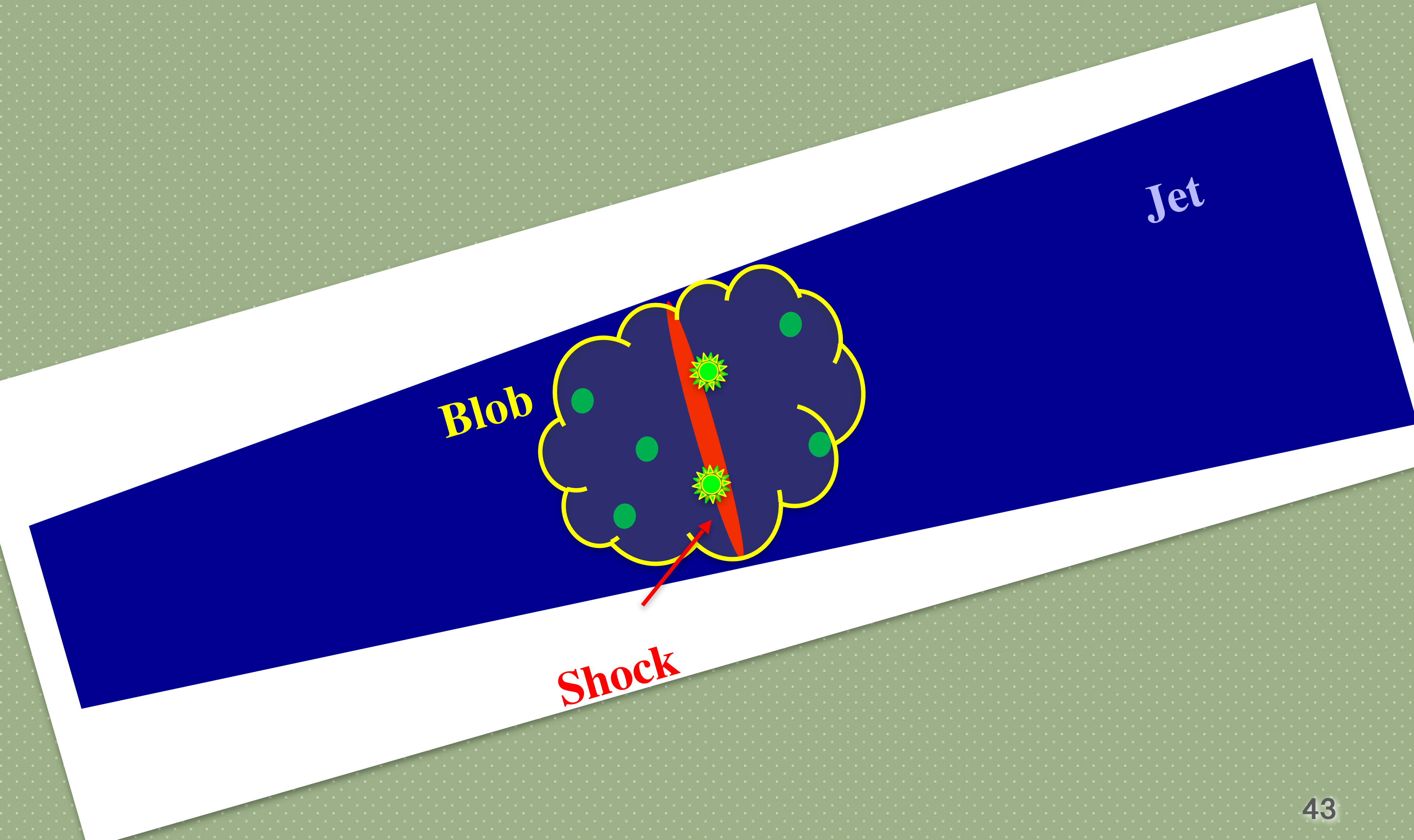

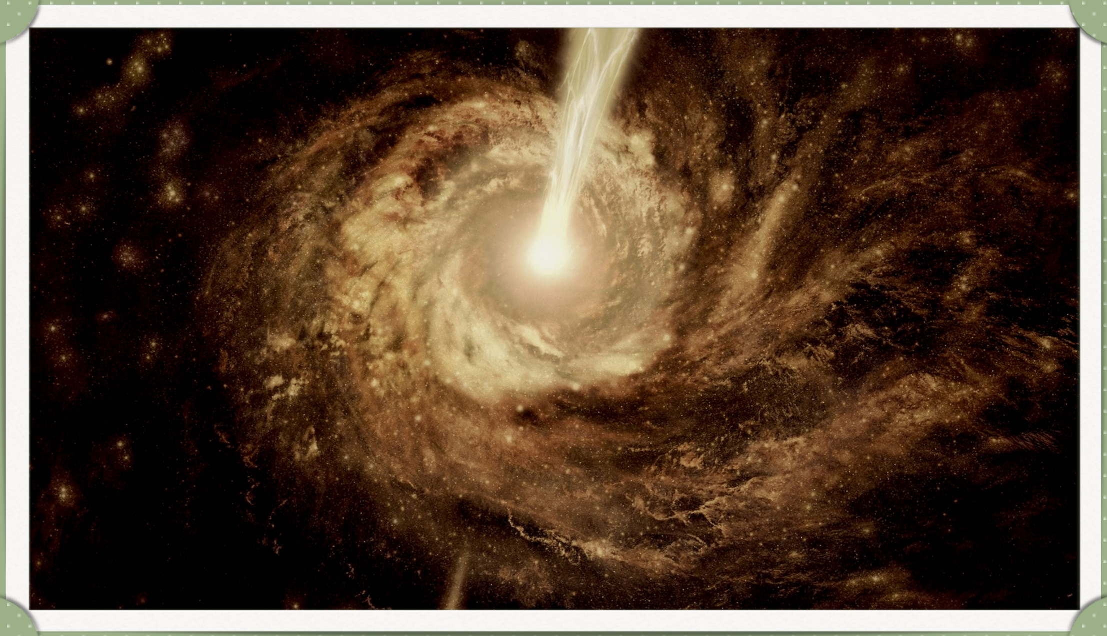

Questions?

Snowmass 2021

The Snowmass Community Planning Process informs DOE, NSF-Physics, and NASA of community driven science and facilities that form major opportunities for fundamental physics over the next decade.

The Future of Gamma-Ray Experiments in the MeV-EeV Range

The Gamma-Ray white paper is asking for Endorsers!

- With full name and orcid (sorry no affiliations)
- Will be listed at the beginning of the document, under the editors
- May also be section authors (which are listed with their section(s))
- Show support for the science expressed in the document and the community that pursues it

Endorsements and Feedback are collected here (the arxiv link to the paper is in the form):

https://docs.google.com/forms/d/e/1FAIpQLSc9fw0R8pp2RMEQ6wr8Yt7QH_ShfHskA0qNNsF5-MMer-eSIw/viewform?usp=sf_link

Thanks for your support of Future Gamma-Ray Science!

Snowmass 2021

The Snowmass Community Planning Process informs DOE, NSF-Physics, and NASA of community driven science and facilities that form major opportunities for fundamental physics over the next decade.

Advancing the Landscape of Multimessenger Science in the Next Decade

The Multimessenger white paper is asking for Endorsers!

- With full name and orcid (sorry no affiliations)
- Will be listed at the beginning of the document, under the editors and contributors
- Show support for the science expressed in the document and the communities that pursue it

Endorsements and Feedback are collected here (the arxiv link to the paper is in the form):

https://docs.google.com/forms/d/e/1FAIpQLScvdffF7bPRTfAEkmMQEirDcfYUEo4vYxbNOR-4FLxdAy75AA/viewform?usp=sf_link

Thanks for your support for the advancement of Multimessenger Science!